NASA TECHNICAL MEMORANDUM

NASA TM X-2313

NASA TM X-2313

LARGE-SCALE WIND-TUNNEL TESTS OF A PROPELLER-DRIVEN DEFLECTED SLIPSTREAM STOL MODEL IN GROUND EFFECT

by V. Robert Page and Thomas N. Aiken

Ames Research Center

Moffett Field, Calif. 94035

NATIONAL AERONAUTICS AND SPACE ADMINISTRATION • WASHINGTON, D. C. • OCTOBER 1971

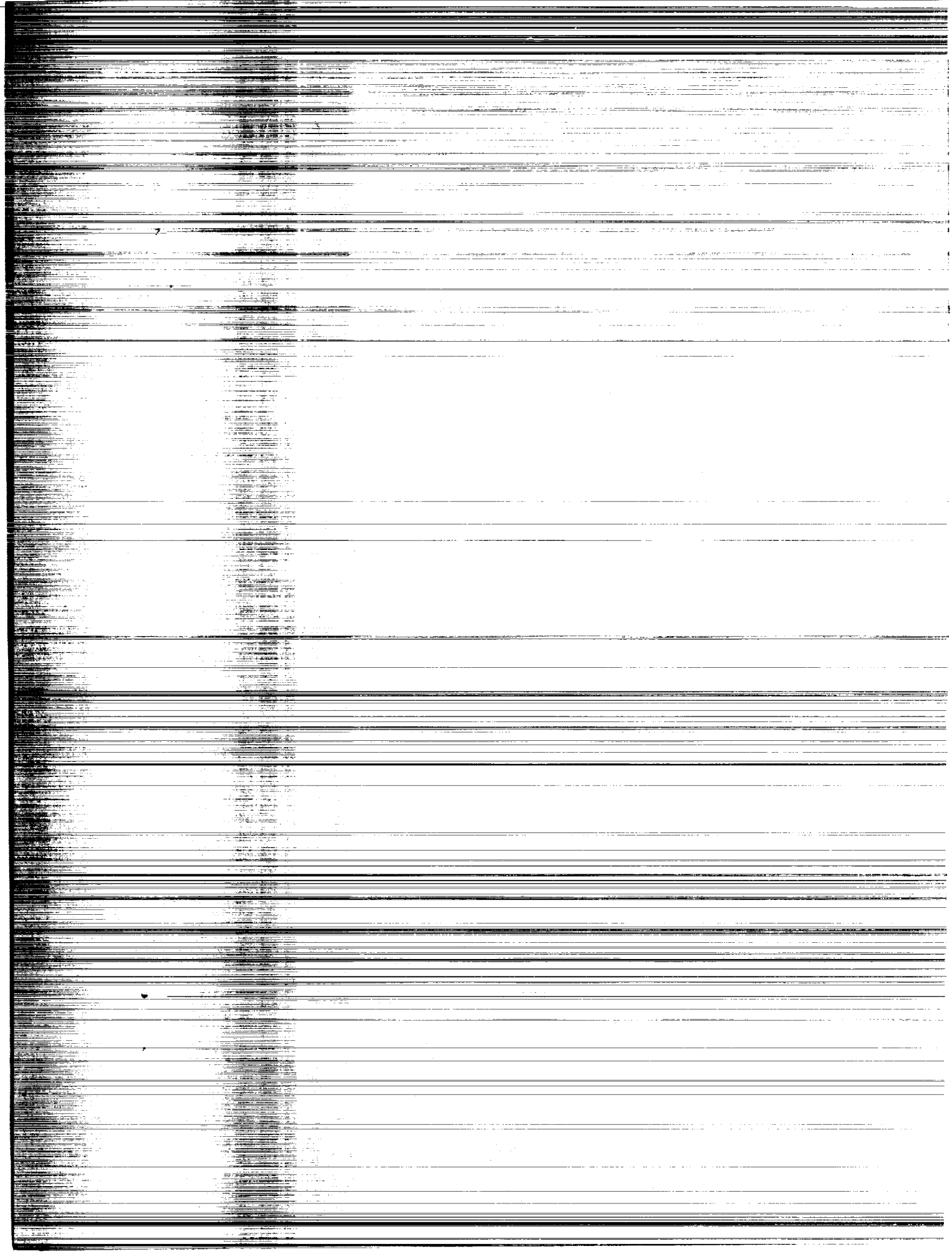

1. Report No.	2. Government Accession No.	3. Recipient's Catalog No.
NASA TM X-2313		

4. Title and Subtitle	5. Report Date
LARGE-SCALE WIND-TUNNEL TESTS OF PROPELLER-DRIVEN DEFLECTED SLIPSTREAM STOL MODEL IN GROUND EFFECT	October 1971
	6. Performing Organization Code

7. Author(s)	8. Performing Organization Report No.
V. Robert Page and Thomas N. Aiken	A-3927
	10. Work Unit No.
9. Performing Organization Name and Address	721-60-10-05-00-21
Ames Research Center Moffett Field, Calif., 94035	11. Contract or Grant No.
	13. Type of Report and Period Covered
12. Sponsoring Agency Name and Address	Technical Memorandum
National Aeronautics and Space Administration Washington, D. C. 20546	14. Sponsoring Agency Code

15. Supplementary Notes

16. Abstract

A wind-tunnel investigation was conducted to determine the longitudinal and lateral-directional characteristics of a large-scale STOL transport model in ground effect. Test configurations included three wing spans (aspect ratios, 5.71, 6.52, and 8.06), with and without full-span triple-slotted trailing-edge flaps, horizontal tail on and off, spanwise variation of propeller thrust (to vary the span loading and descent capability), differential propeller pitch for yaw control, and spoiler and slot-lip aileron for roll control. All tests were made with the mean aerodynamic chord of the wing 3.76 m (12.33 ft) ($h/\bar{c} \approx 1.6$) above the floor of the test section. The test data are presented without analysis.

17. Key Words (Suggested by Author(s))	18. Distribution Statement
Propeller STOL Deflected slipstream High-lift wings	Unclassified – Unlimited

19. Security Classif. (of this report)	20. Security Classif. (of this page)	21. No. of Pages	22. Price*
Unclassified	Unclassified	43	$3.00

*For sale by the National Technical Information Service, Springfield, Virginia 22151

NOTATION

b	wing span, m (ft), and blade width, cm (in.)
c	wing chord parallel to fuselage center line, m (ft)
$\bar{c}$	mean aerodynamic chord, $\frac{2}{S}\int_0^{b/2} c^2\, dy$, m (ft)
C_D	drag coefficient including thrust, $\frac{\text{measured drag}}{qS}$
C_L	lift coefficient including thrust, $\frac{\text{measured lift}}{qS}$
c_{L_d}	propeller blade design lift coefficient
C_l	rolling-moment coefficient, $\frac{\text{rolling moment}}{qSb}$
C_m	pitching-moment coefficient, $\frac{\text{pitching moment}}{qS\bar{c}}$
C_n	yawing-moment coefficient, $\frac{\text{yawing moment}}{qSb}$
C_y	side-force coefficient, $\frac{\text{side force}}{qS}$
D	propeller diameter, m (ft)
J	propeller advance ratio, $\frac{V}{nD}$
L	lift including thrust component, n (lb)
n	propeller rotational velocity, rps
q_∞	free-stream dynamic pressure, n/sq m (lb/sq ft)
R	Reynolds number, $\rho \frac{V\bar{c}}{\mu}$
r	propeller blade radius, m (ft)
S	wing area, sq m (sq ft)
T	total thrust of all four propellers, n (lb)

t	propeller blade thickness, cm (in.)
T_c'	thrust coefficient, $\frac{T}{qS}$
V	free-stream velocity, m/sec (fps)
WRP	wing reference plane
x	distance aft of local wing chord leading edge, percent chord
y	distance above or below wing reference plane, percent chord; or lateral distance spanwise from fuselage centerline, m (ft)
α	angle of attack of fuselage reference line, deg
β	propeller blade angle at 0.75 r, deg
$\frac{\beta xx}{xx}$	blade angle at 0.75 r for inboard/outboard propellers, respectively, deg
β x/x/x/x	blade angle at 0.75 r for propellers 1/2/3/4 (pilots view of engines left to right), respectively, deg
δ_f	total aft flap deflection relative to local wing chord, deg
$\delta\frac{xx}{xx}$	differential spanwise flap deflection where numerator is for flap extents inboard of midpoint between nacelles and denominator is for flap extents outboard (e.g., δ_f 100/60 = 100° inboard/60° outboard)
δ_s	spoiler deflection, deg
δ_{sla}	slot-lip aileron deflection, deg
η	wing semispan station, $\frac{2y}{b}$
μ	coefficient of viscosity, n sec/m^2 (slugs/ft sec)
ρ	mass density of air, kg/m^3 (slugs/ft^3)
ψ	angle of yaw, deg

LARGE–SCALE WIND–TUNNEL TESTS OF A PROPELLER–DRIVEN DEFLECTED SLIPSTREAM STOL MODEL IN GROUND EFFECT

V. Robert Page and Thomas N. Aiken

Ames Research Center

SUMMARY

A wind-tunnel investigation was conducted to determine the longitudinal and lateral-directional characteristics of a large-scale STOL transport model in ground effect. Test configurations included three wing spans (aspect ratios, 5.71, 6.52, and 8.06), with and without full-span triple-slotted trailing-edge flaps, horizontal tail on and off, spanwise variation of propeller thrust (to vary the span loading and descent capability), differential propeller pitch for yaw control, and spoiler and slot-lip aileron for roll control. All tests were made with the mean aerodynamic chord of the wing 3.76 m (12.33 ft) ($h/\bar{c} \approx 1.6$) above the floor of the test section. The test data are presented without analysis.

INTRODUCTION

The longitudinal and lateral-directional characteristics of a propeller-driven deflected-slipstream STOL model in ground effect were investigated as part of a continuing study of this model. The model was tested previously, out of ground effect, with the tail off (refs. 1 and 2) and with the tail on (ref. 3).

The objectives of this investigation were (1) to determine the longitudinal characteristics in ground effect, and (2) to explore thoroughly the lateral-directional characteristics through high angles of yaw for a typical landing configuration. The 100/60 flap deflection was chosen as a typical landing configuration because in reference 3 it was concluded that although a uniform spanwise flap deflection of 80° was more efficient and allowed better descent angles, directional stability appeared to increase with higher inboard and lesser outboard flap deflections.

MODEL AND APPARATUS

Figure 1 is a photograph of the model installed in the 40– by 80–foot wind tunnel test section.

The airfoil section of the wing was an NACA 63_2–416 without the reflex on the aft portion of the lower surface. Coordinates of the wing, leading-edge slat and trailing-edge triple-slotted flap are presented in reference 1. The wing and tail geometry is given in table 1.

The wing as shown in figure 1 had a span of 17.06 m (56 ft) and an aspect ratio of 8.06. With the shorter tips the span was 14.61 m (47.94 ft) and the aspect ratio 6.52. Without tips the span was 13.21 m (43.34 ft) and the aspect ratio 5.71 (fig. 2(a)).

A cross section of the wing leading-edge slat and trailing-edge triple-slotted flap is shown in figure 2(b). The trailing-edge flap could be deflected 100° with respect to the wing chord line. For flap deflections of 80° or less, the foreflap was set at half the total deflection of the aft flap. For a flap deflection of 100°, the foreflap was deflected 40°.

A cross section view of the slot-lip aileron and spoiler is shown in figure 2(c). The slot-lip aileron was 0.10 wing chord and was tested with a 0.10 wing chord extension. The slot-lip aileron was located aft of the 0.6 wing chord station, outboard of the inboard nacelle ($\eta = 0.385 \rightarrow 1.0$) on the short wing. The spoiler was 0.10 wing chord and was located aft of the 0.6 wing chord station, outboard of the midpoint ($\eta = 0.57 - 1.0$) between the nacelles.

The geometric characteristics of the three-bladed model propellers are presented in figure 3. The solid aluminum model propellers had a diameter of 2.84 m (9.3 ft) and an activity factor of 121 per blade. Each propeller was shaft mounted on a gear box and driven by an electric motor. The four motors were operated in parallel from a variable frequency power supply.

TEST PROCEDURE AND CORRECTIONS

Tests were made at free-stream velocities of 12 to 25 m/sec (34 to 49 knots) corresponding to Reynolds numbers from 2.7 to 4.1 million based on mean aerodynamic chords of 2.2 to 2.4 m (7.3 to 7.8 ft). For the "longitudinal data" the model angle of attack was varied while the tunnel dynamic pressure, propeller speed, and propeller blade angle were held fixed. Propeller thrust variation with advance ratio is presented in figure 4. For the lateral-directional data the model angle of attack was fixed and only angle of yaw was varied. For runs with all propellers set for equal thrust, the propeller blades were set at angles of 16° at the three-quarter radius station. To obtain differential spanwise thrust the inboard propeller blade angle was left at 16° while the outboard propeller blade angle was set at 0°. With this blade setting, and assuming inboard thrust to be independent of outboard thrust, the two inboard propellers produced a high positive value of thrust while the two outboard propellers gave a slightly negative value. Differential propeller pitch was investigated as a lateral-directional control and obtained by a differential setting of 4° between propellers 1 and 4 with the two inboard propeller blade angles remaining at 16°. This setting was then held for runs at the same nominal motor speeds and tunnel pressures as when the data for equal thrust were taken.

Aerodynamic coefficients were based on the flaps-retracted reference wing area for each of the three wing spans evaluated. Pitching-moment coefficients were computed about a moment center at 0.25 $\bar{c}$.

Wind-tunnel wall corrections were not applied because of the proximity of the ground. An average drag tare correction of 0.02 was applied to account for the drag of the exposed struts.

DATA PRESENTATION

The data are in three parts: (1) longitudinal data for the long span wing (fig. 5), (2) longitudinal data for the medium span wing (figs. 6–9), and (3) lateral-directional data (figs. 10–13) for the short span wing. Table 2 is an index to these data. All test configurations were run at the same elevation in the wind-tunnel test section.

The longitudinal characteristics of the long span wing without slats are presented in figure 5 for several flap deflections and with the horizontal tail in the low position. Figures 6 and 7 present the longitudinal data of the medium span wing, with an without full-span slats for several flap deflections, and with the horizontal tail in the low position. Figure 8 presents data for the latter configuration minus the horizontal tail. Figure 9 shows the effect of differential spanwise thrust (β = 16/0) on the medium span wing, with slats off, and the tail in the low position. Figures 10 to 13 present the lateral-directional data (tail off) for the short span wing for a landing flap configuration of 100/60. The four figures show data taken at angles of yaw from -8° to +31° and at 0° angle of attack. The results show the effects of slats, differential propeller pitch, slot-lip aileron and spoiler, respectively.

Ames Research Center
National Aeronautics and Space Administration
Moffett Field, Calif., 94035, June 28, 1971

1. Page, V. Robert; Dickinson, Stanley O.; and Deckert, Wallace H.: Large-Scale Wind-Tunnel Tests of a Deflected Slipstream STOL Model With Wings of Various Aspect Ratios. NASA TN D–4448, 1968.

2. Page, V. Robert; and Soderman, Paul T.: Wing Surface Pressure Data From Large-Scale Wind-Tunnel Tests of a Propeller-Driven STOL Model. NASA TM X–1527, 1968.

3. Page, V. Robert; and Aiken, Thomas N.: Stability and Control Characteristics of a Large-Scale Deflected Slipstream STOL Model With a Wing of 5.7 Aspect Ratio. NASA TN D–6393, 1971.

TABLE 1.– MODEL GEOMETRY

Dimension	Wing span			Vertical tail	Horizontal tail
	Short	Medium	Long		
Area, sq m (sq ft)	30.6(329)	32.8(352.8)	36.2(389.3)	8.08(86.9)	11.79(126.9)
Span, m (ft)	13.21(43.34)	14.61(47.94)	17.06(56)	3.42(11.22)	6.3(20.65)
Mean aerodynamic chord, m (ft)	2.38(7.80)	2.32(7.62)	2.22(7.30)	2.52(8.26)	1.91(6.26)
Aspect ratio	5.71	6.52	8.06	1.45	3.36
Taper ratio	0.554	0.507	0.424	0.389	0.612
Twist, deg	0	0	0	0	0
Dihedral, deg	0	0	0	0	0
NACA airfoil section	63_2–416	63_2–416	63_2–416	63A013	Inverted 63A212
Sweep of leading edge, deg	2.88	2.88	2.88	31.33	15.98
Sweep of trailing edge, deg	-8.57	-8.57	-8.57	0	0
Root chord, m (ft)	2.98(9.77)	2.98(9.77)	2.98(9.77)	3.40(11.17)	2.32(7.62)
Tip chord, m (ft)	1.65(5.41	1.51(4.95)	1.26(4.14)	1.32(4.34)	1.42(4.66)

TABLE 2.– FIGURE INDEX

(a) Longitudinal data

Wing span	Slats	Horizontal tail	δ_f, deg	β, deg	Figure
Long	Off	Low, 0°	0	16	5a
↓	↓	↓	40	↓	b
↓	↓	↓	80	↓	c
Medium	Off	Low, 0°	0	↓	6a
↓	↓	↓	40	↓	b
↓	↓	↓	60/40	↓	c
↓	↓	↓	80	↓	d
↓	↓	↓	100/60	↓	e
↓	On	↓	40	↓	7a
↓	↓	↓	80	↓	b
↓	↓	↓	100/60	↓	c
↓	↓	Off	40	↓	8a
↓	↓	↓	80	↓	b
↓	↓	↓	100/60	↓	c
↓	Off	Low, 0°	0	16/0	9a
↓	↓	↓	40	↓	b
↓	↓	↓	60/40	↓	c
↓	↓	↓	80	↓	d
↓	↓	↓	100/60	↓	e

(b) Lateral data. Tail off; $\delta_f = 100/60$

Wing span	Slats	δ_{sla}, deg	δ_s, deg	β, deg	Figure
Short	Off	0	0	16	10a
↓	On	↓	↓	16	b
↓	↓	↓	↓	18/16/16/14	11a
↓	↓	↓	↓	14/16/16/18	b
↓	↓	20	↓	16	12a
↓	↓	60	↓	↓	b
↓	↓	0	20	↓	13a
↓	↓	0	40	↓	b

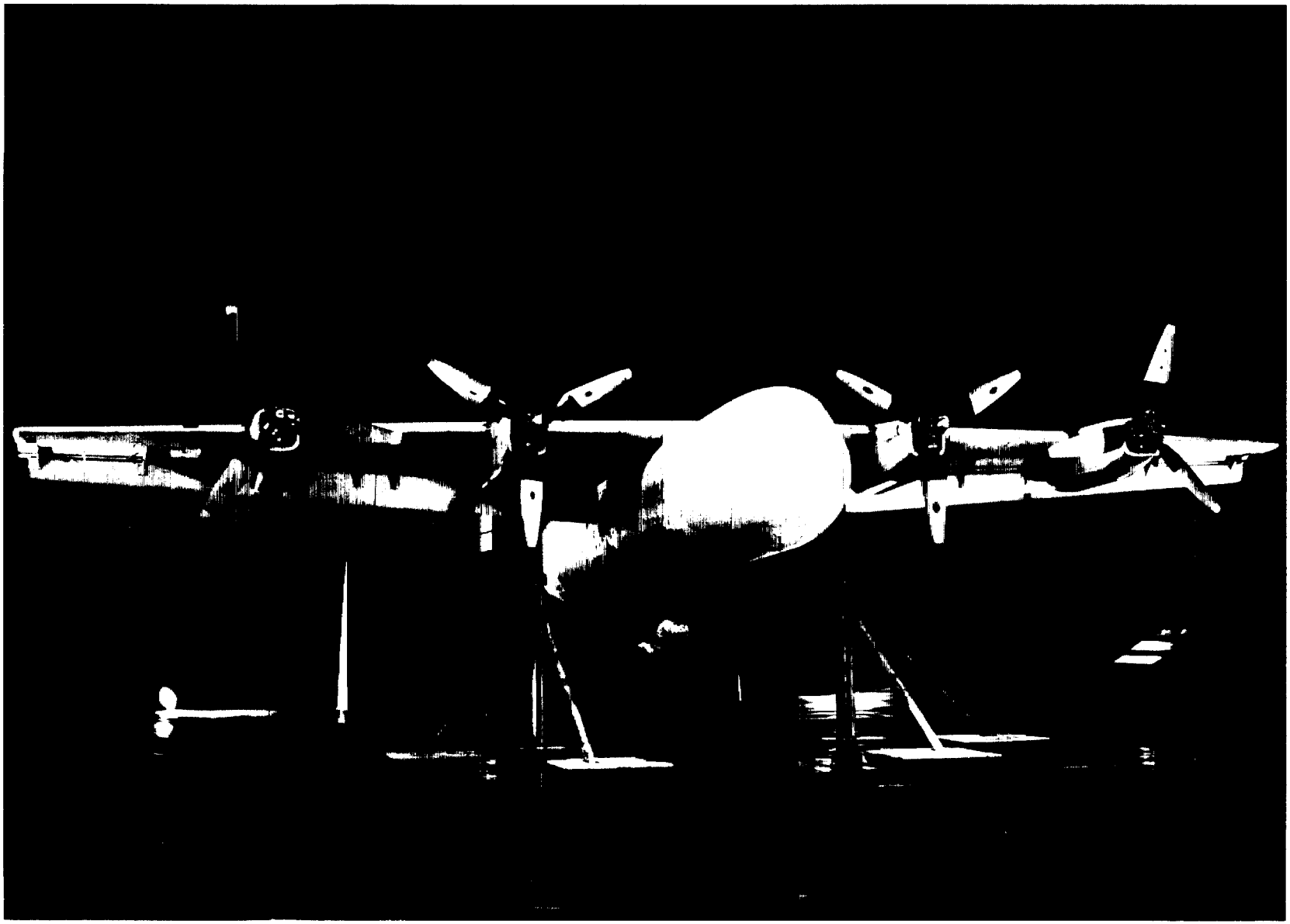

A-39635

Figure 1.- Model with long-span wing in Ames 40– by 80–Foot Wind Tunnel.

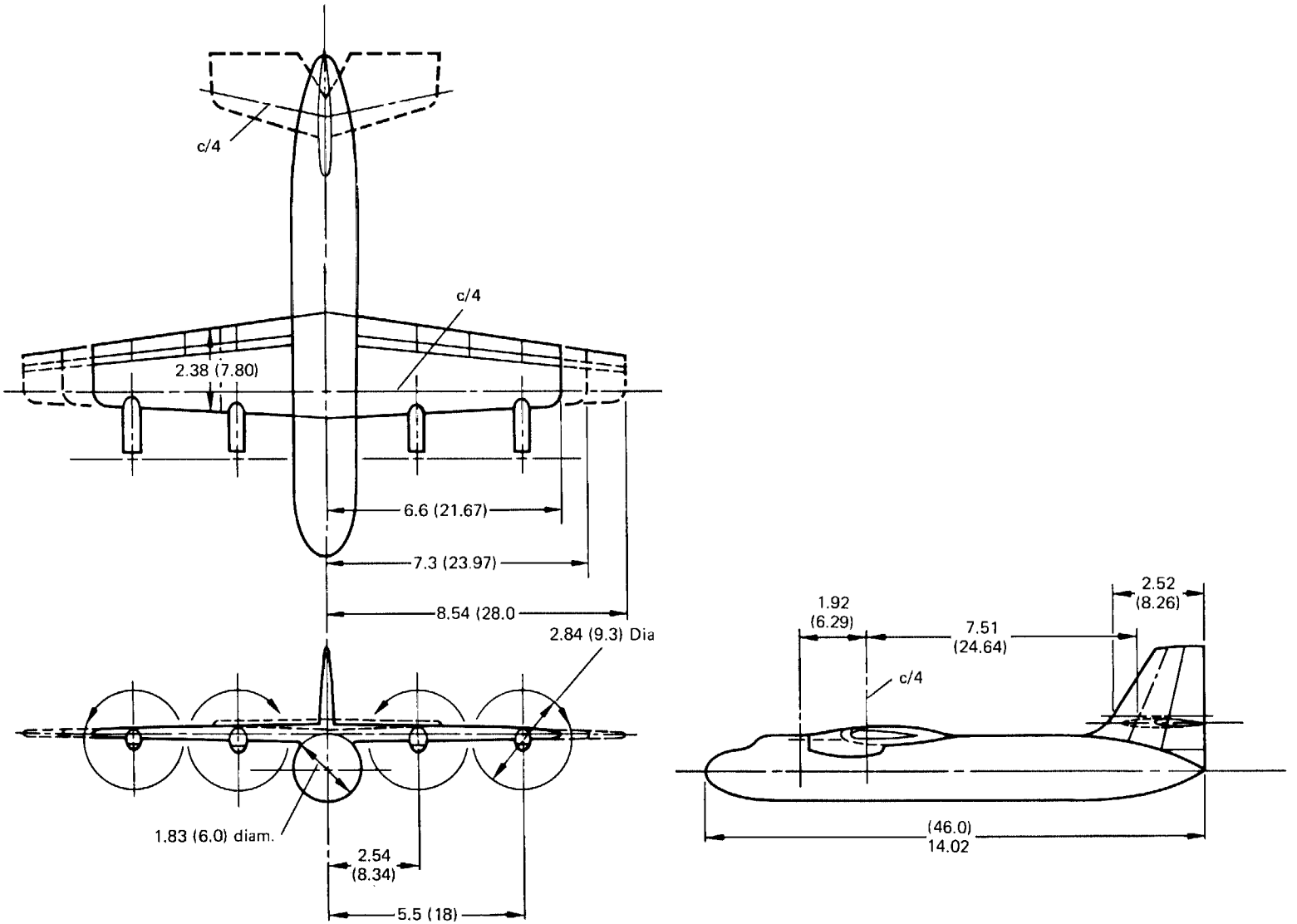

(a) Three-view drawing; dimensions, m (ft).

Figure 2.- Model geometry.

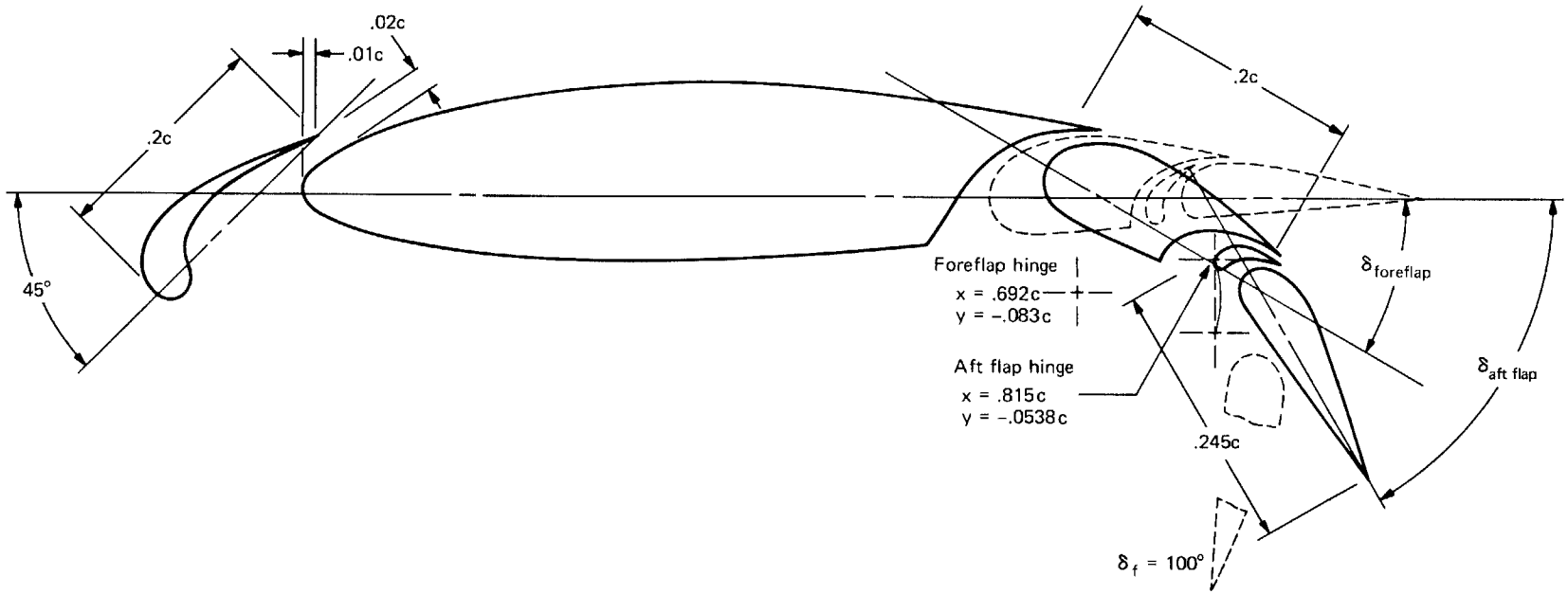

(b) 0.2c slat and triple slotted flap geometry.

Figure 2.- Continued.

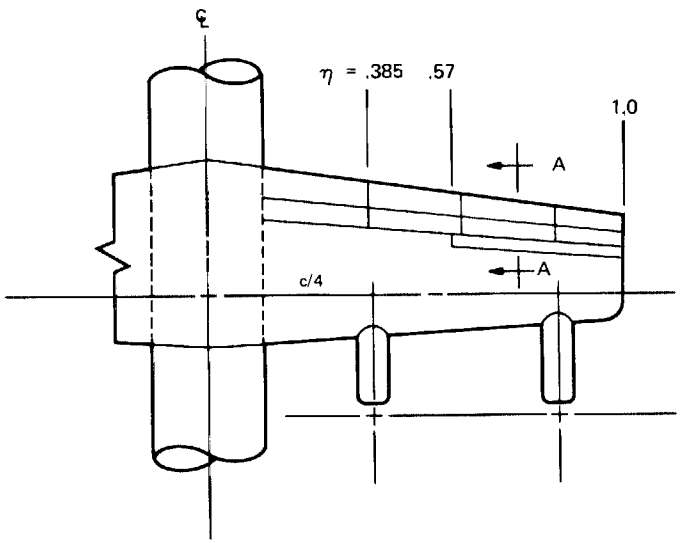

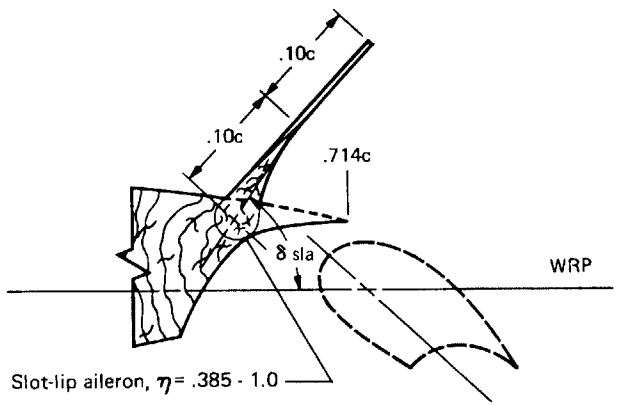

A-A

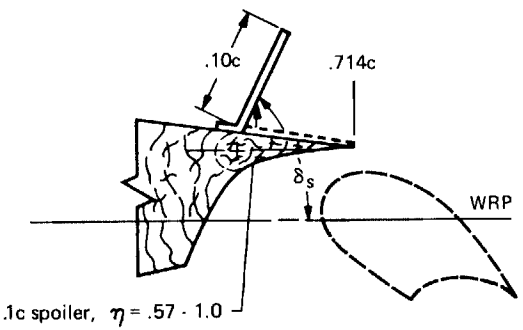

A-A

(c) Spoiler and slot-lip aileron details.

Figure 2.- Concluded.

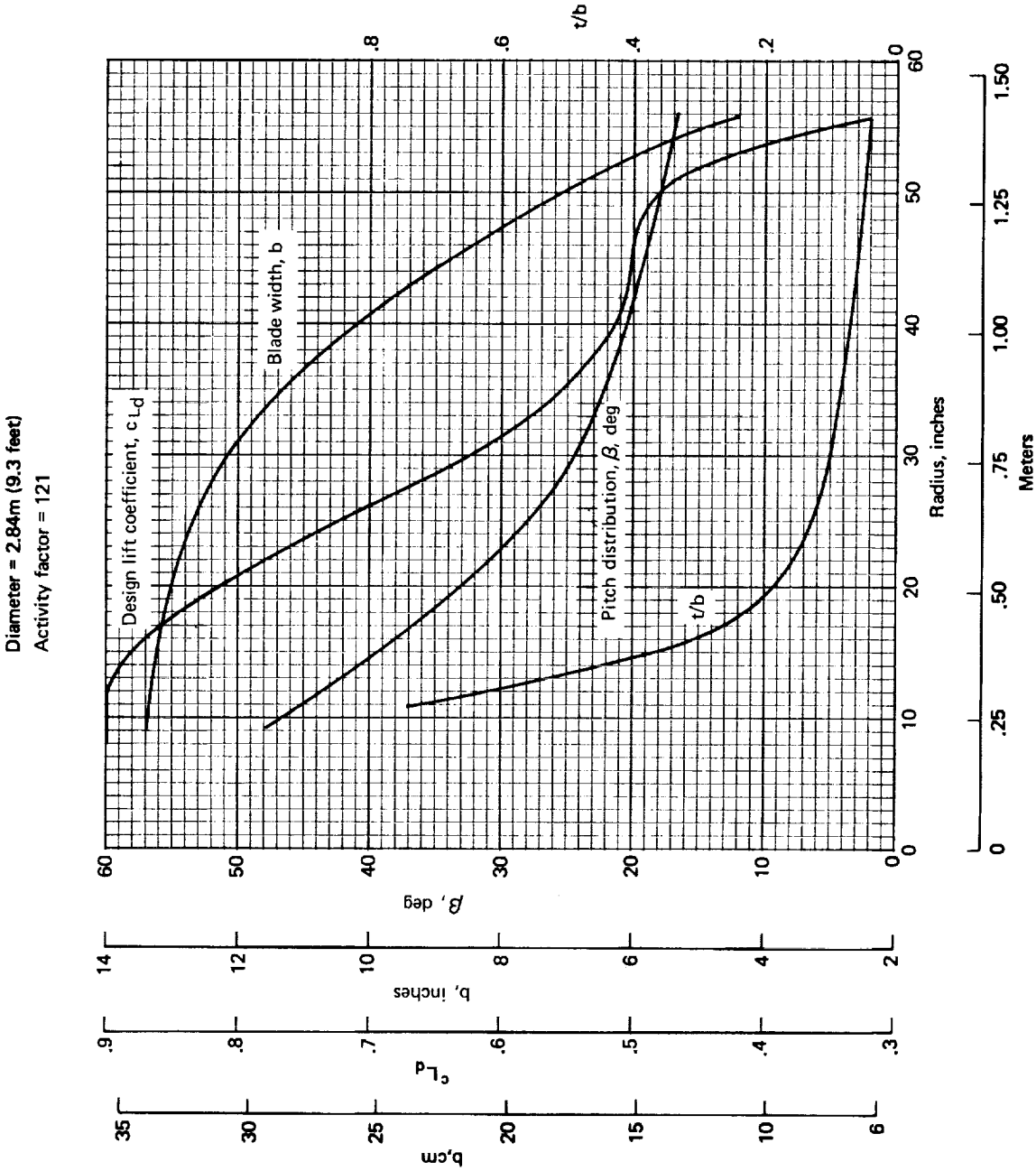

Figure 3.- Blade characteristics for three-blade propeller.

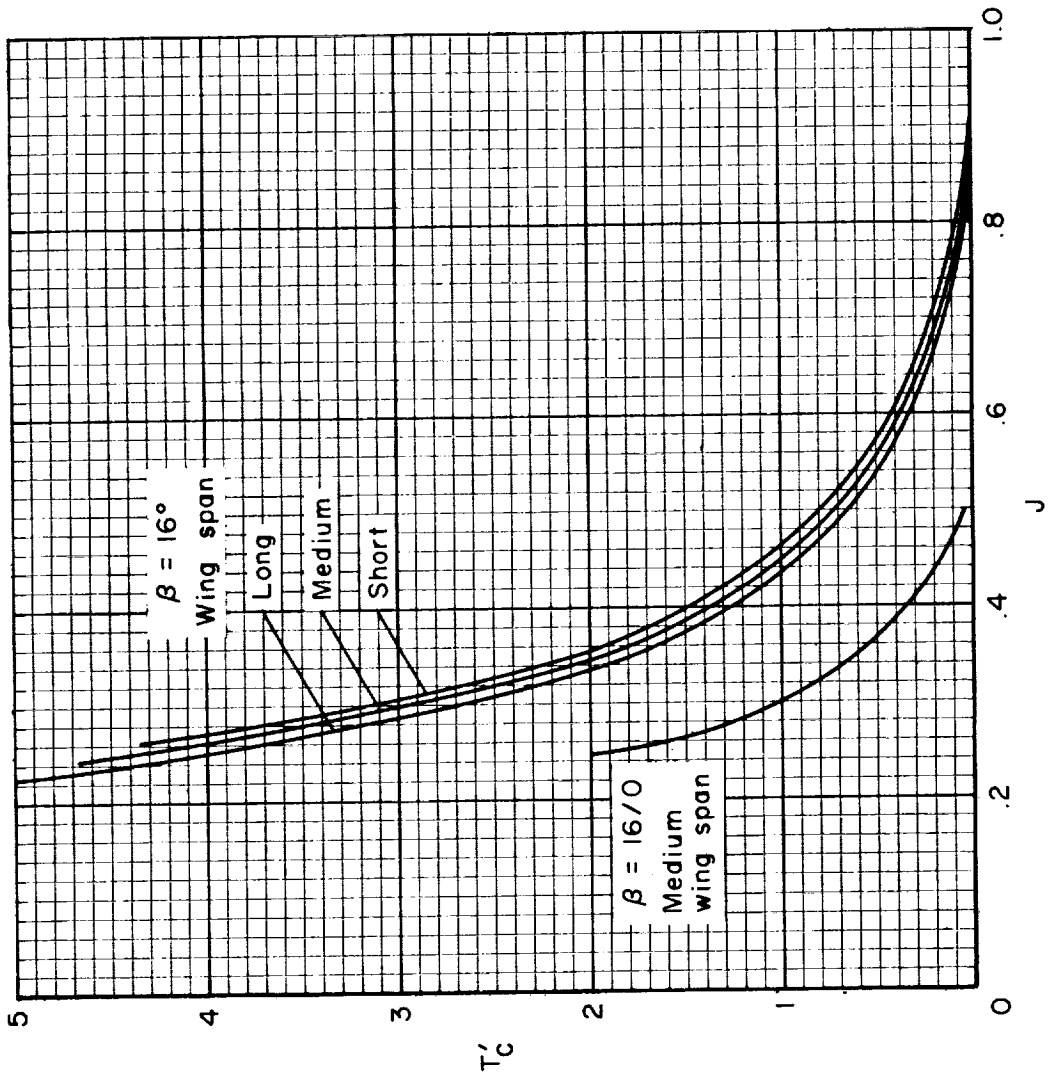

Figure 4.- Variation of propeller thrust coefficient with propeller advance ratio, standard day.

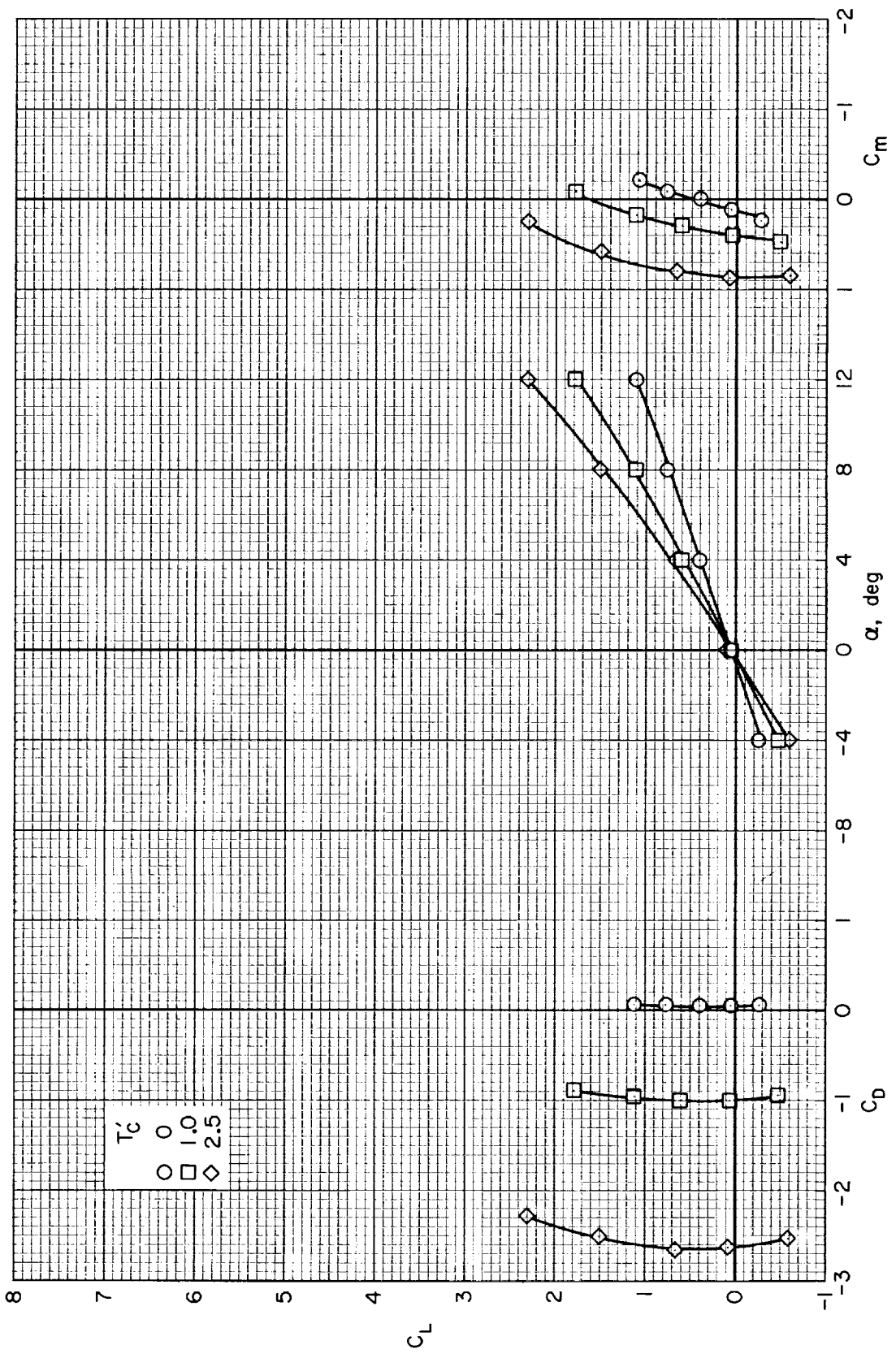

(a) $\delta_f = 0°$

Figure 5.- Longitudinal characteristics of the model with long-span wing, clean leading edge, low horizontal tail; $\beta = 16°$.

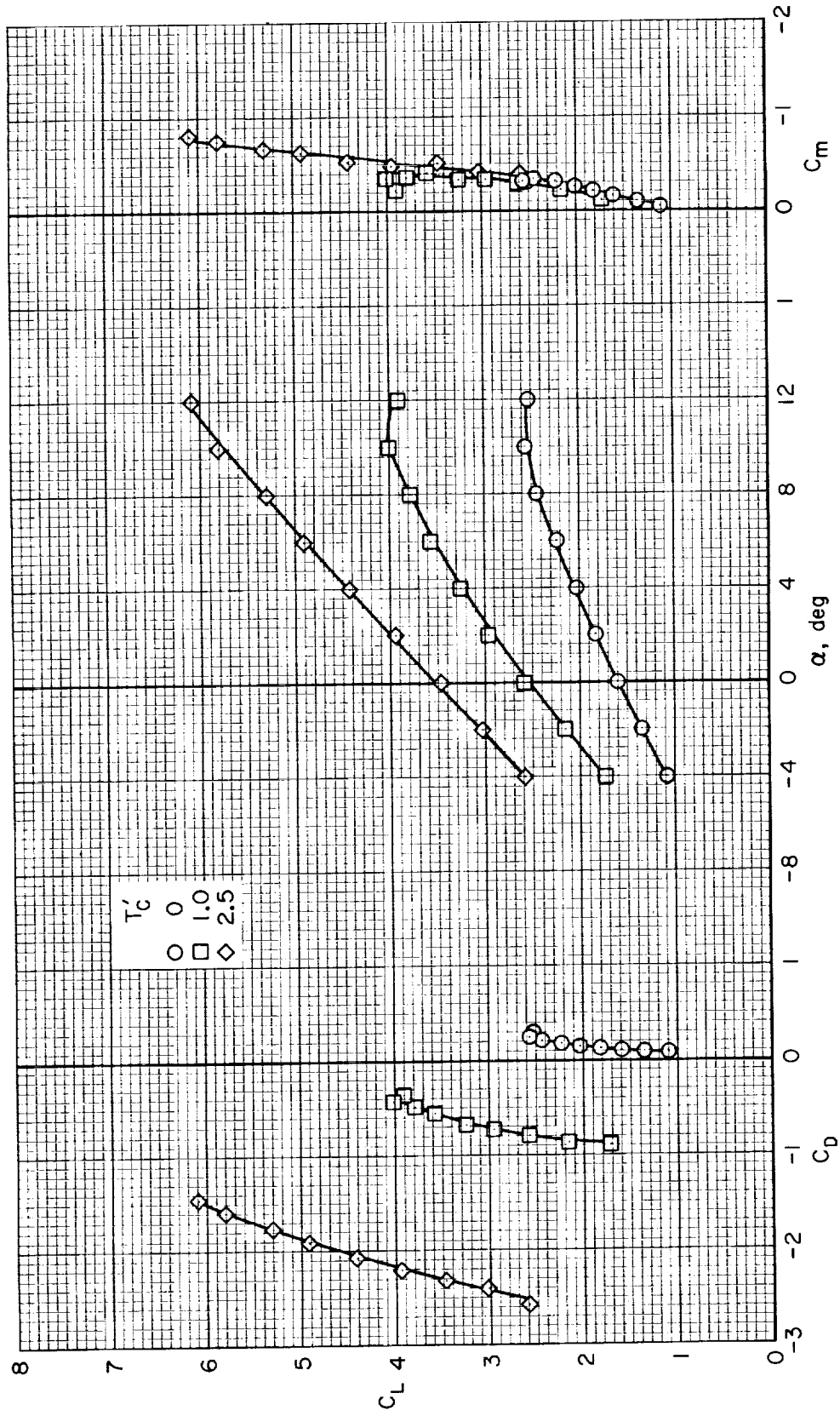

(b) $\delta_f = 40°$

Figure 5.- Continued.

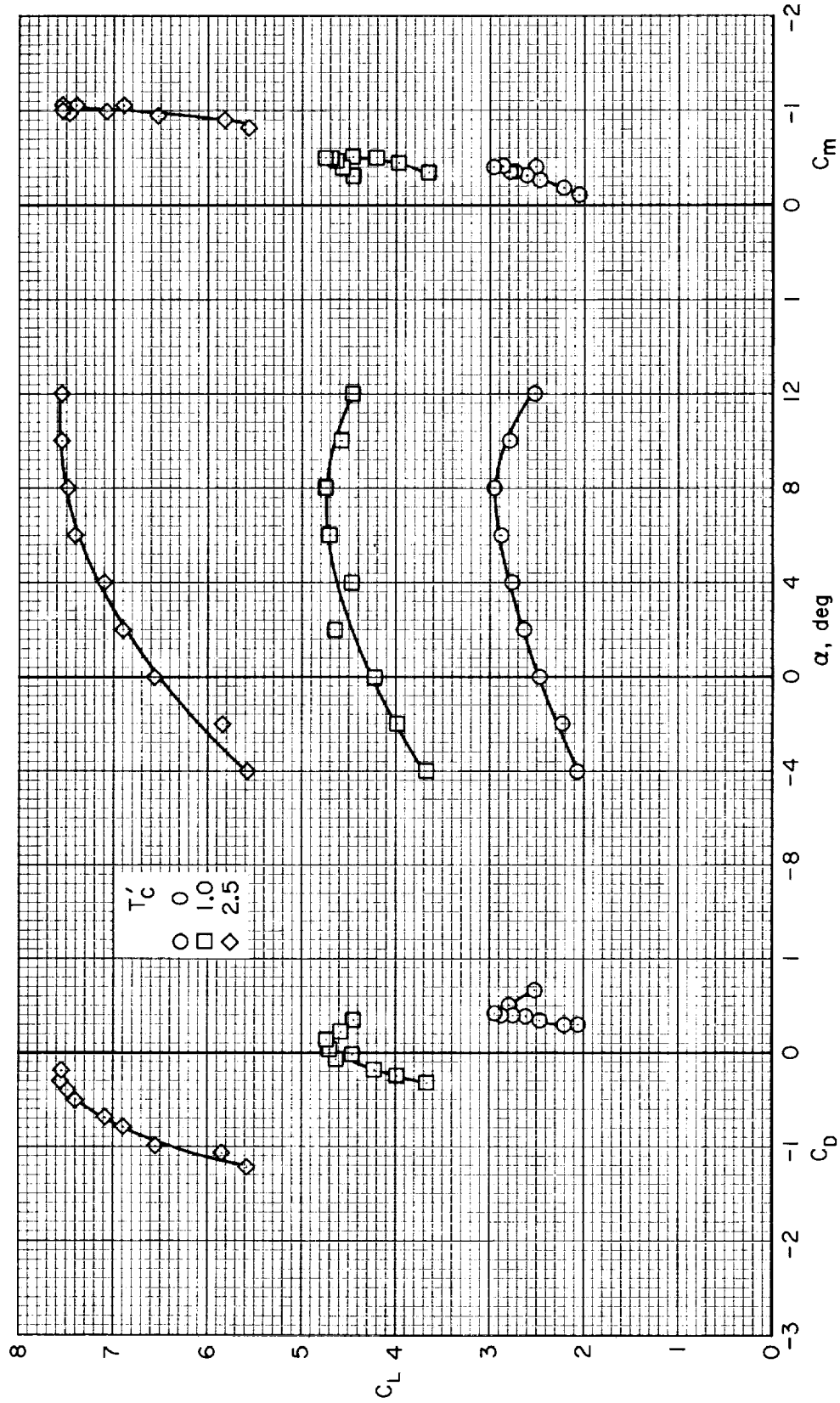

(c) $\delta_f = 80°$

Figure 5.- Concluded.

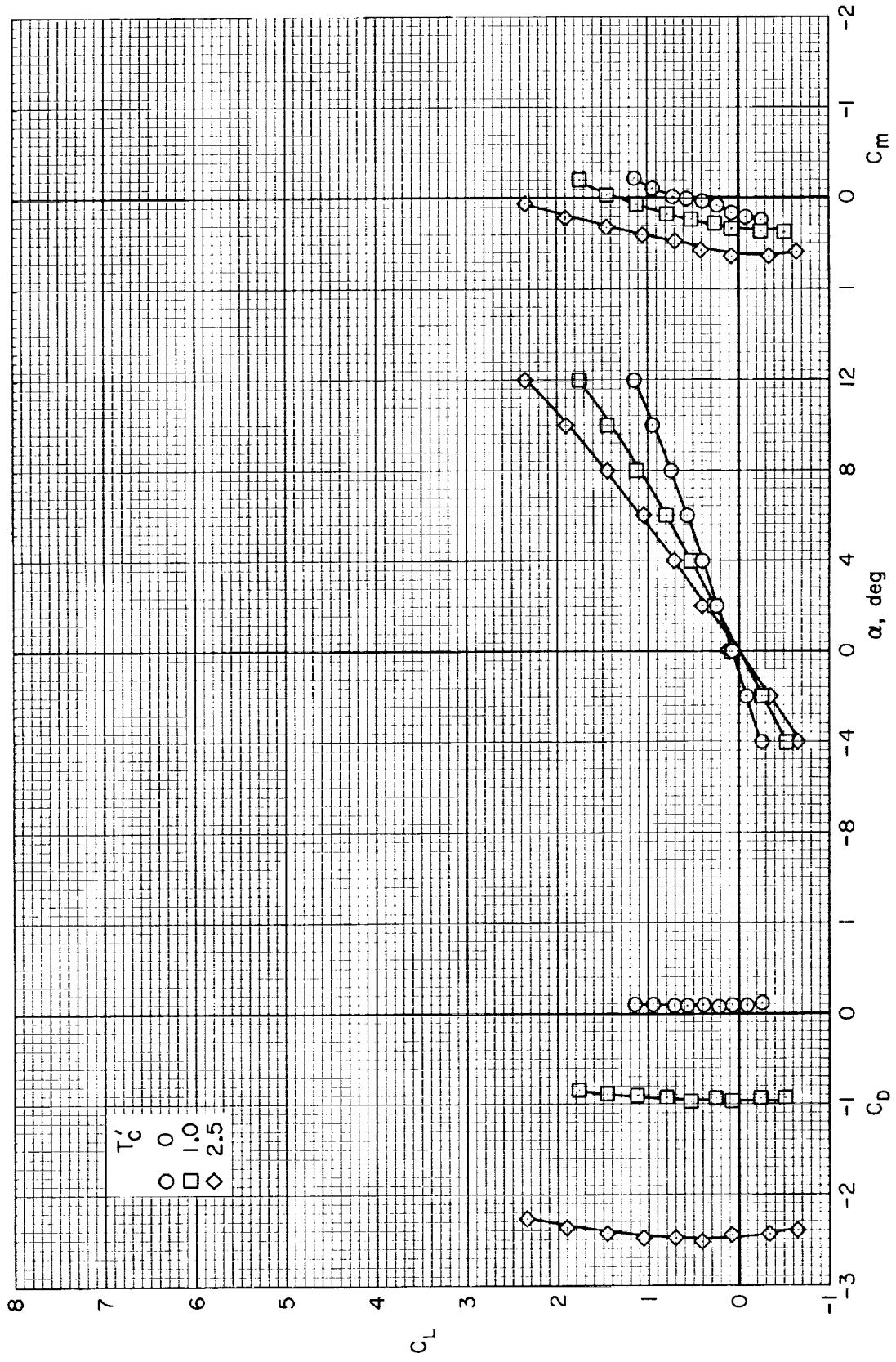

(a) $\delta_f = 0°$

Figure 6.- Longitudinal characteristics of the model with medium-span wing, clean leading edge, low horizontal tail; $\beta = 16°$.

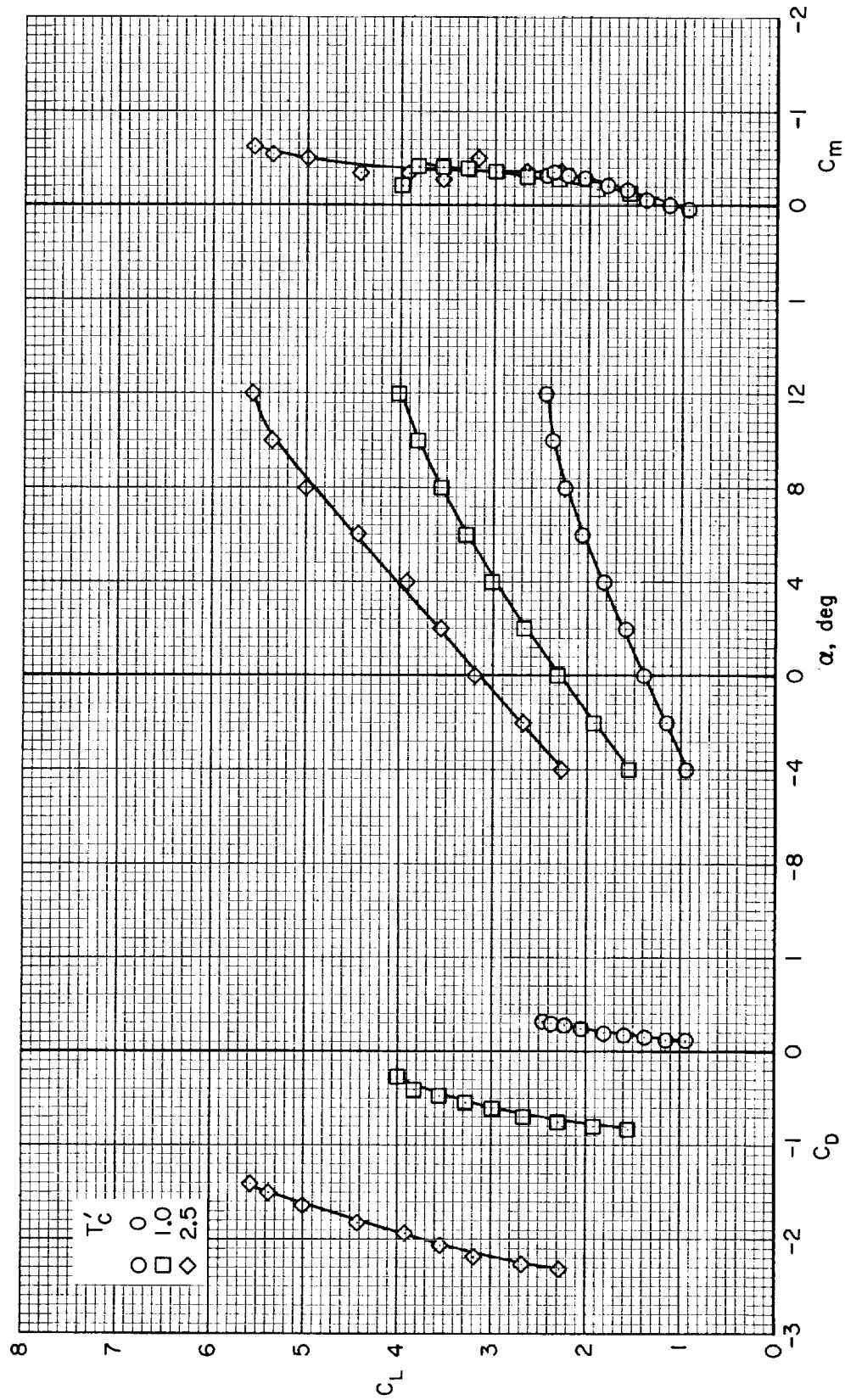

(b) $\delta_f = 40°$

Figure 6.- Continued.

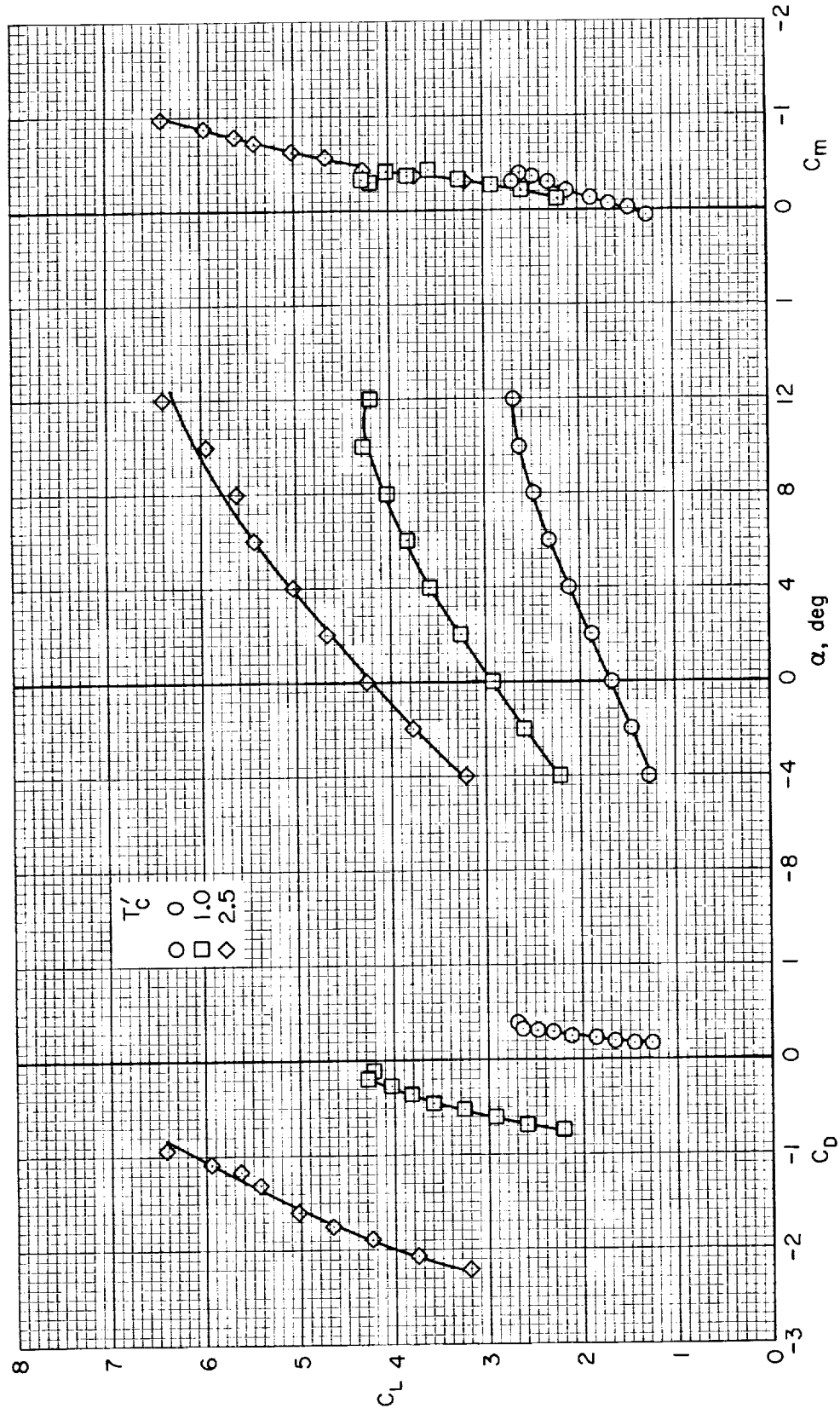

(c) $\delta_f = 60/40°$

Figure 6.- Continued.

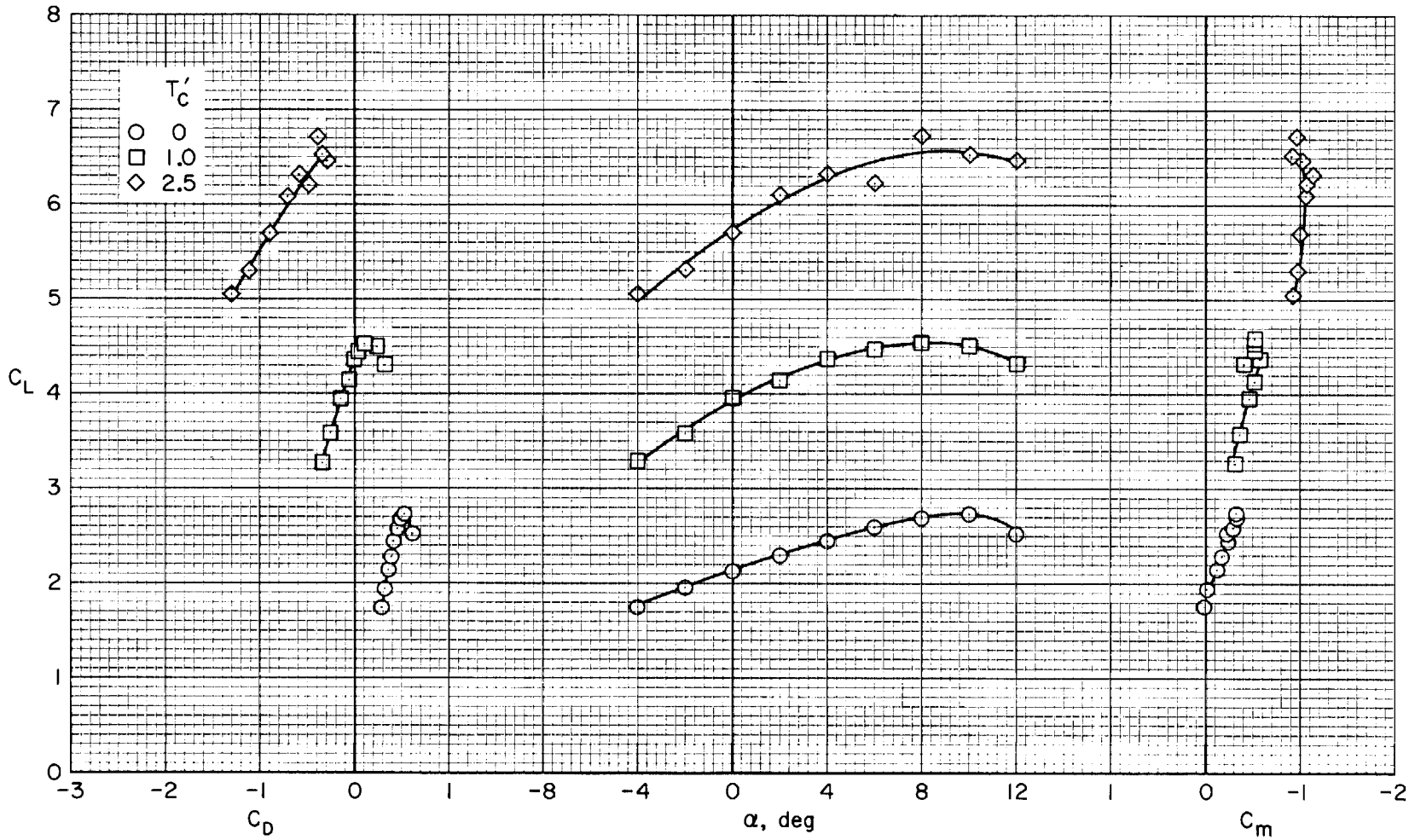

(d) $\delta_f = 80°$

Figure 6.- Continued.

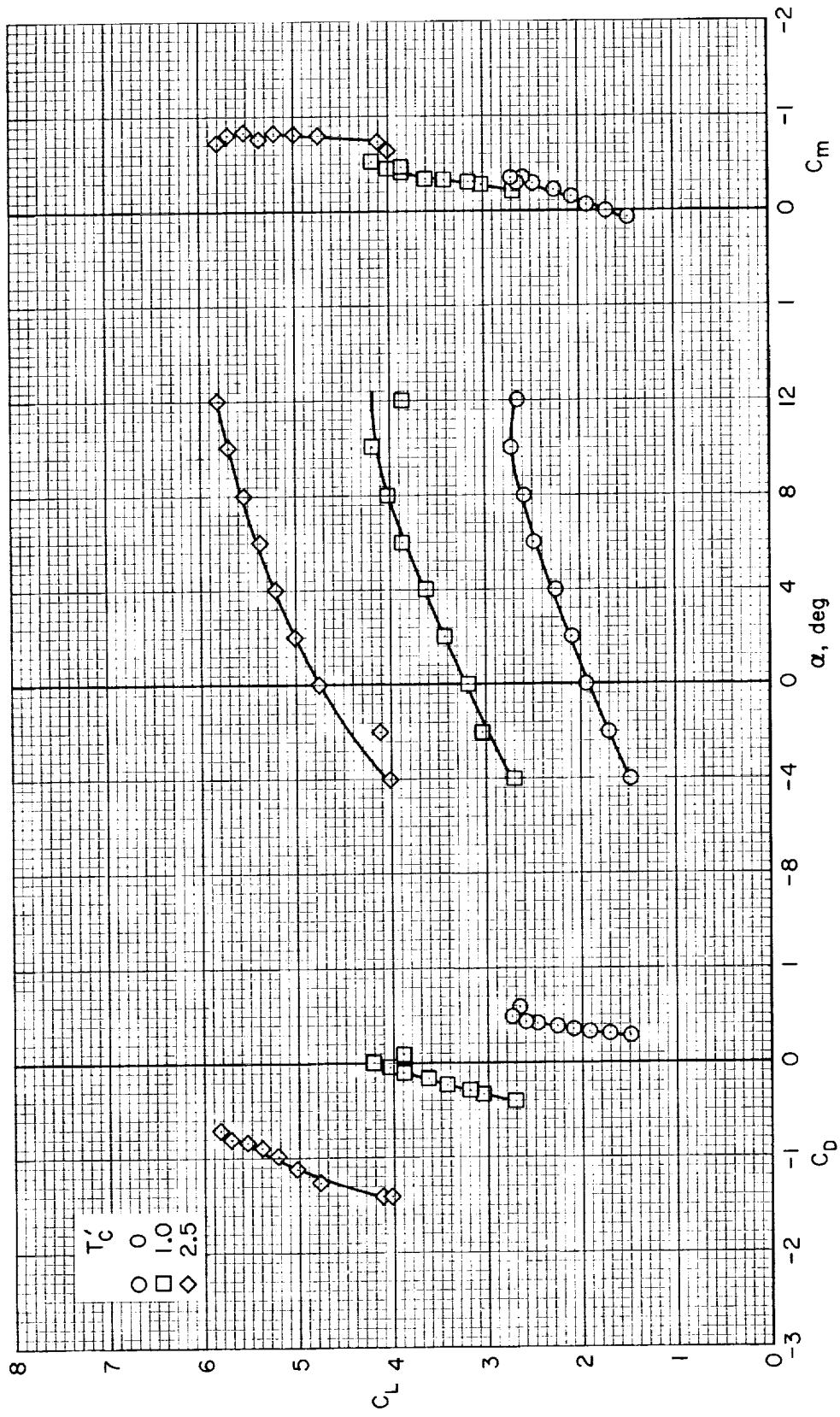

(e) $\delta_f = 100/60°$

Figure 6.- Concluded.

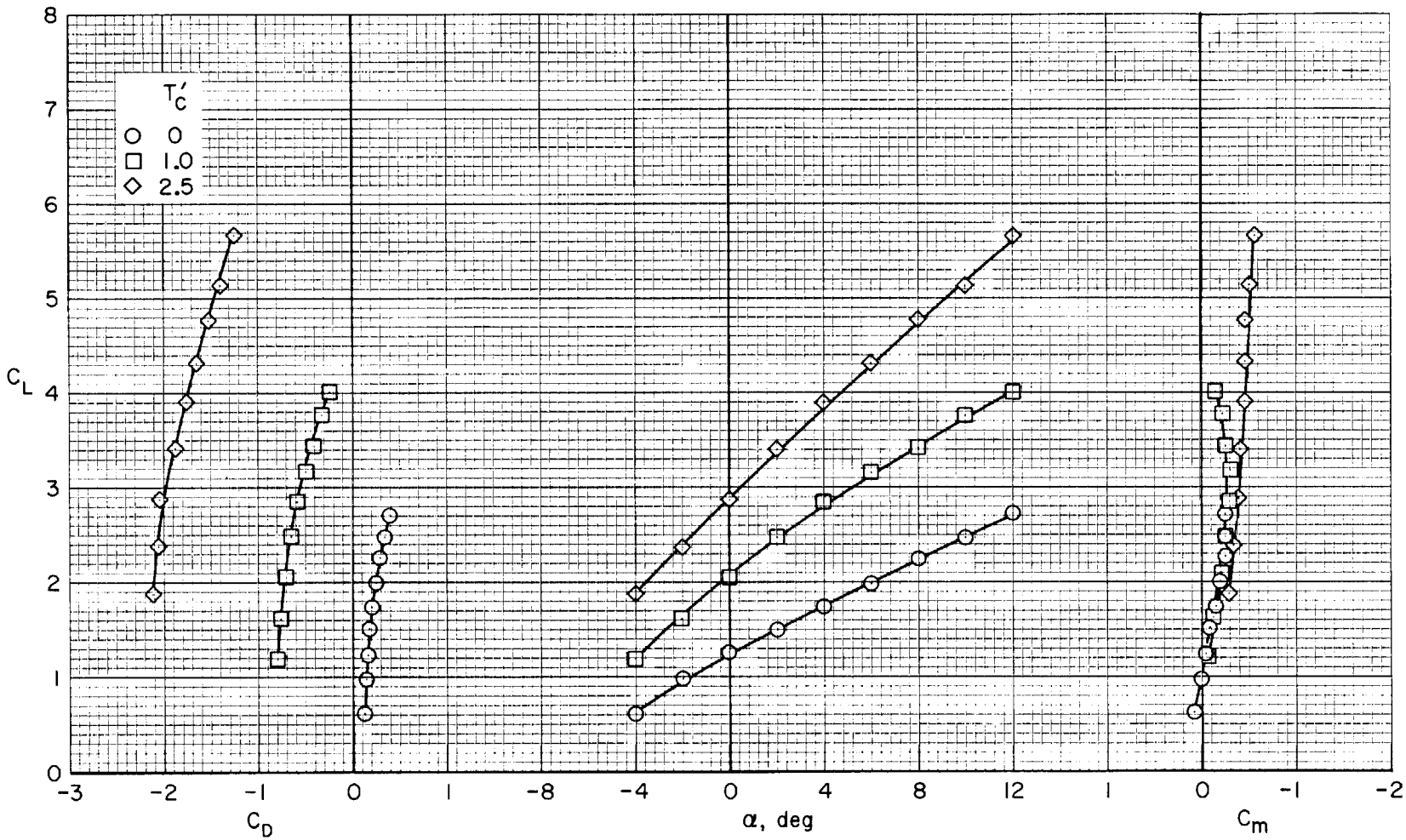

(a) $\delta_f = 40°$

Figure 7.- Effect of leading-edge slats on the longitudinal characteristics of the model with medium-span wing, low tail; $\beta = 16°$.

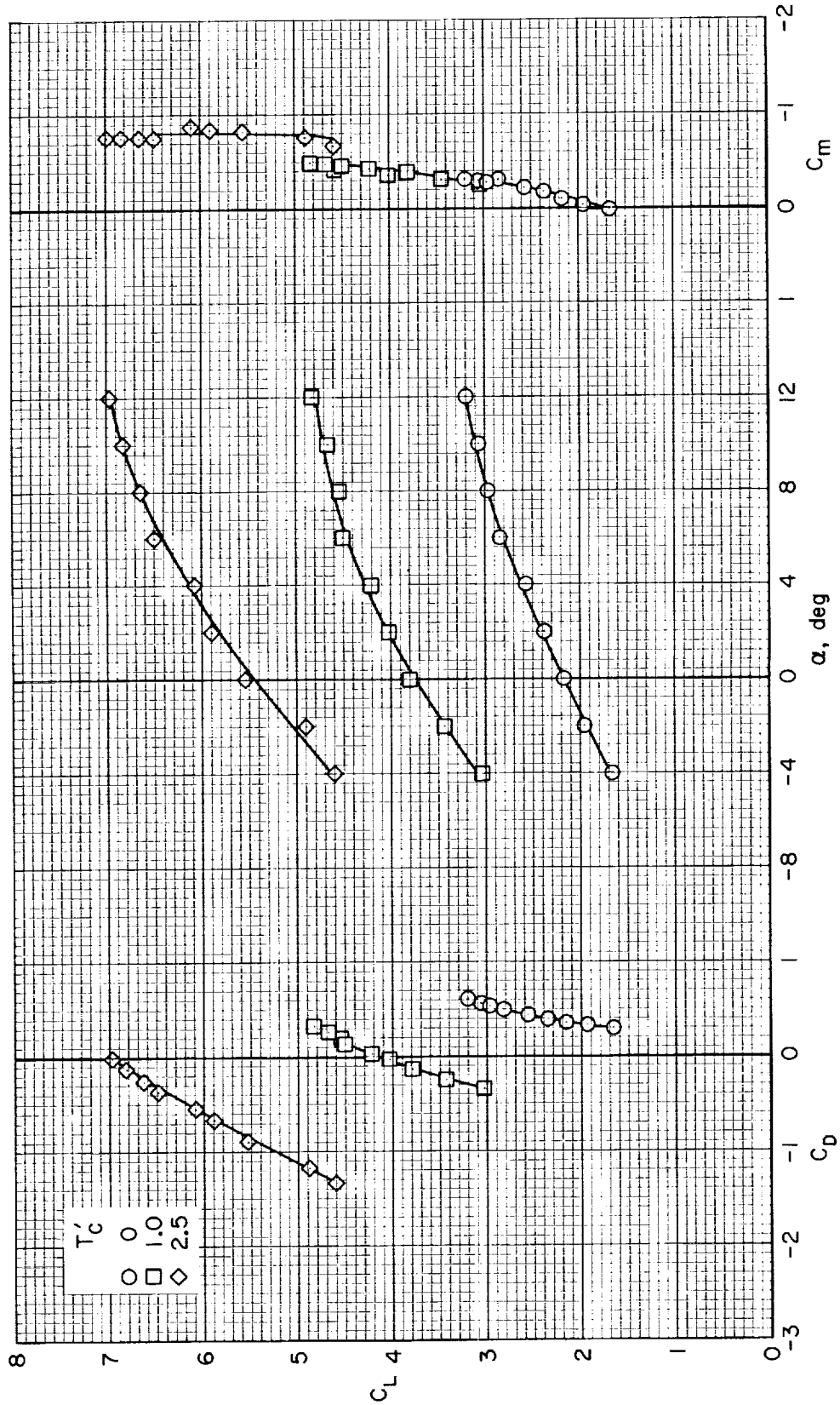

(b) $\delta_f = 80°$

Figure 7.- Continued.

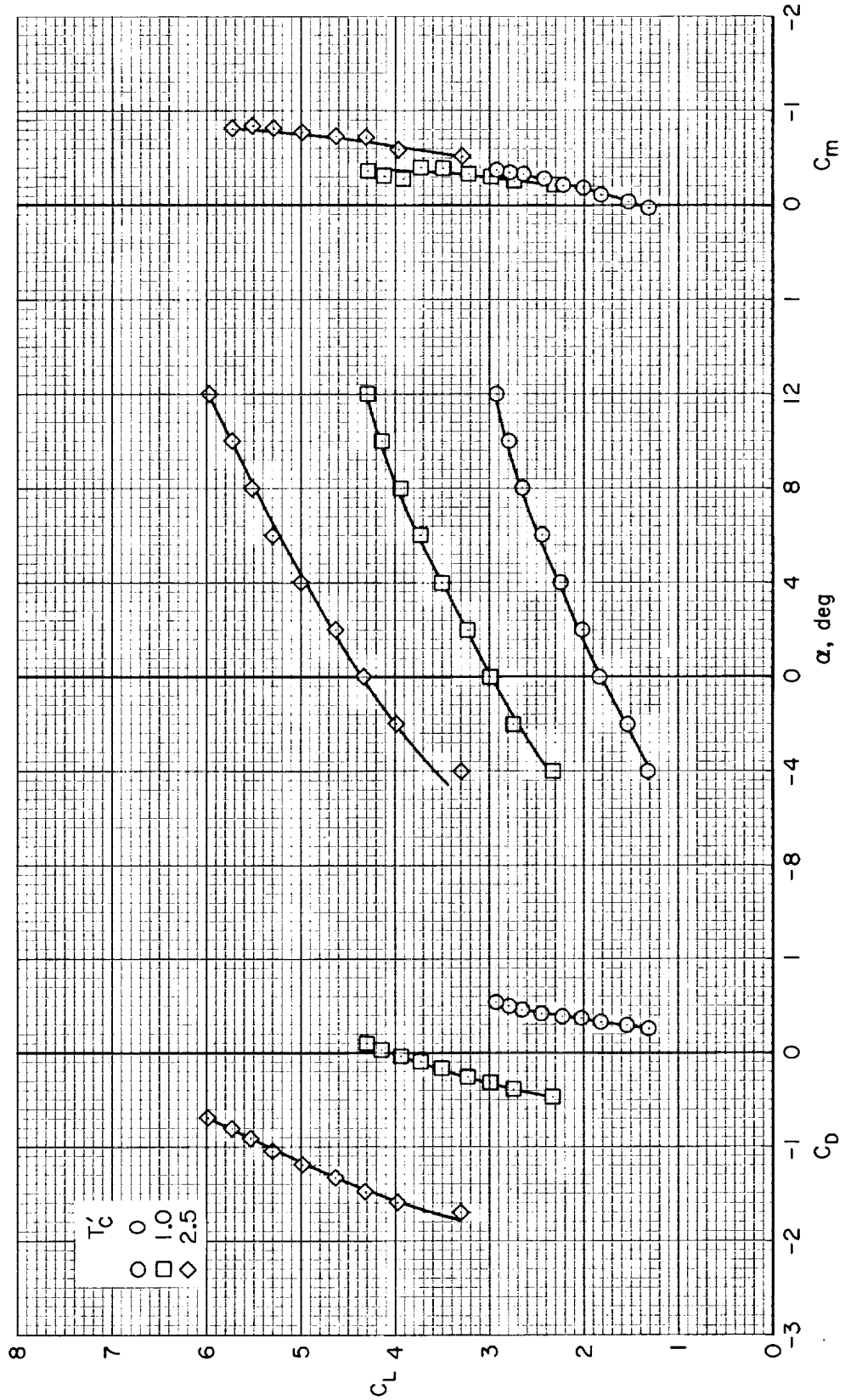

(c) $\delta_f = 100/60°$

Figure 7.- Concluded.

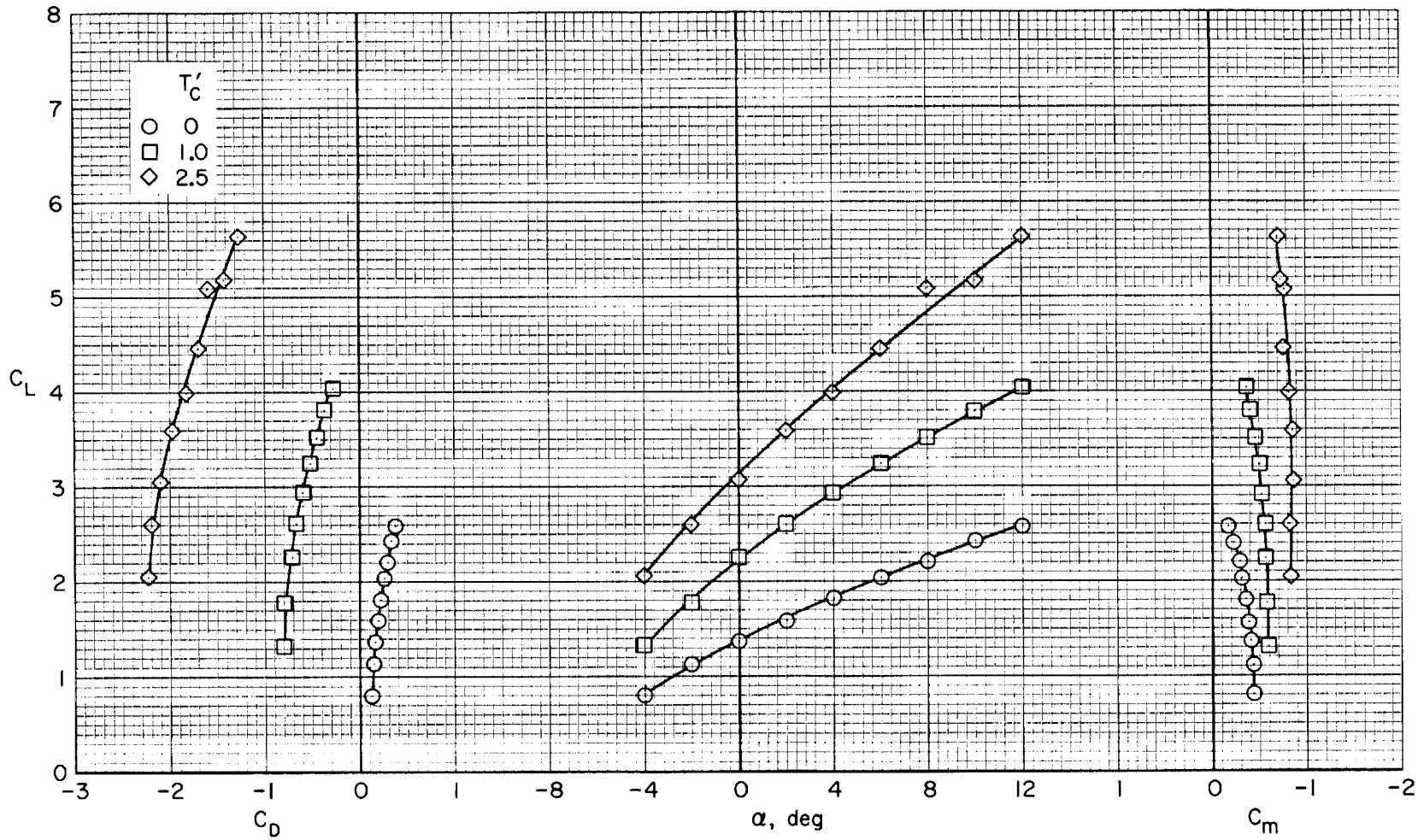

(a) $\delta_f = 40°$

Figure 8.- Longitudinal characteristics of the model with horizontal tail off, medium span wing, full span leading-edge slats; $\beta = 16°$.

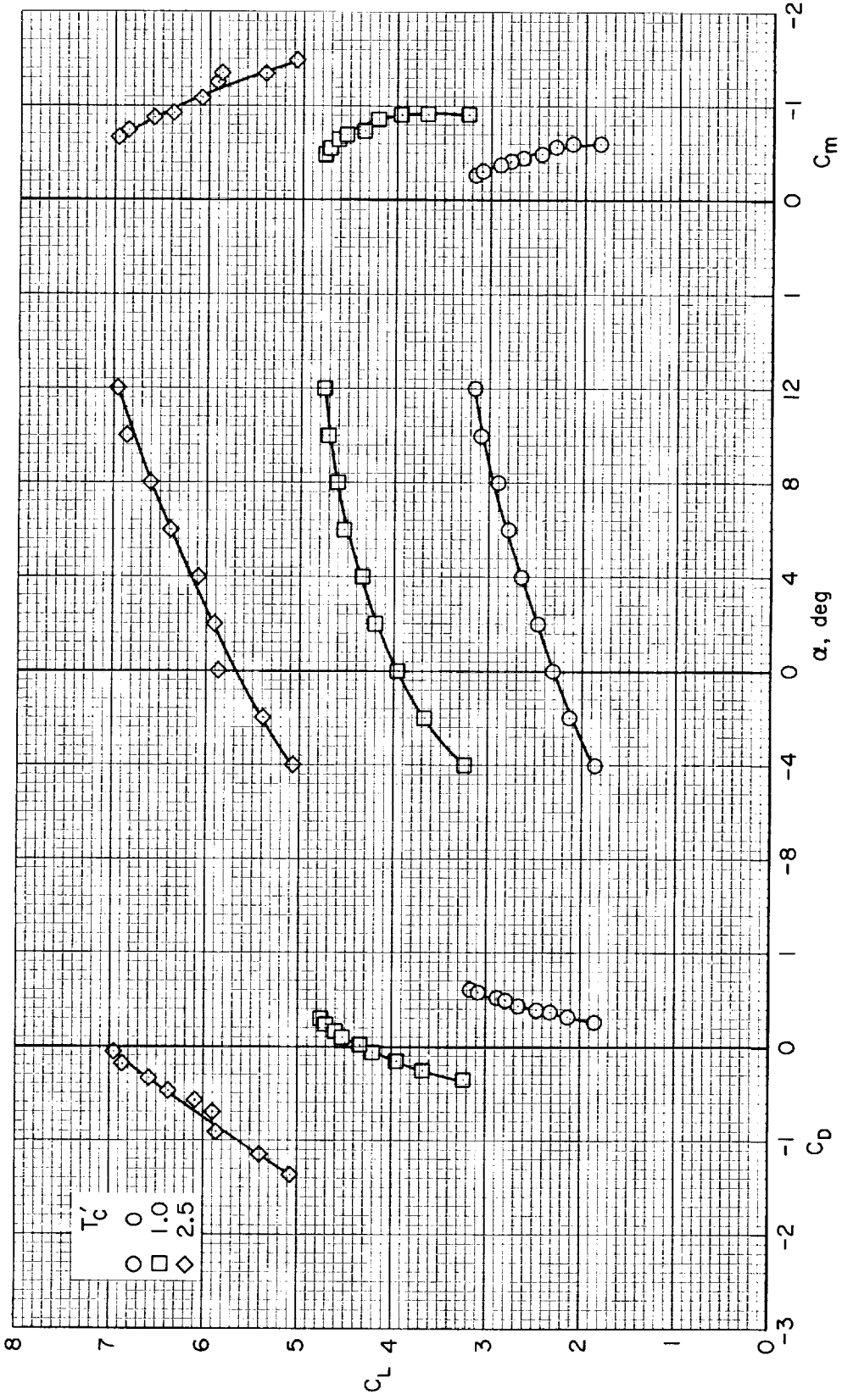

(b) $\delta_f = 80°$

Figure 8.- Continued.

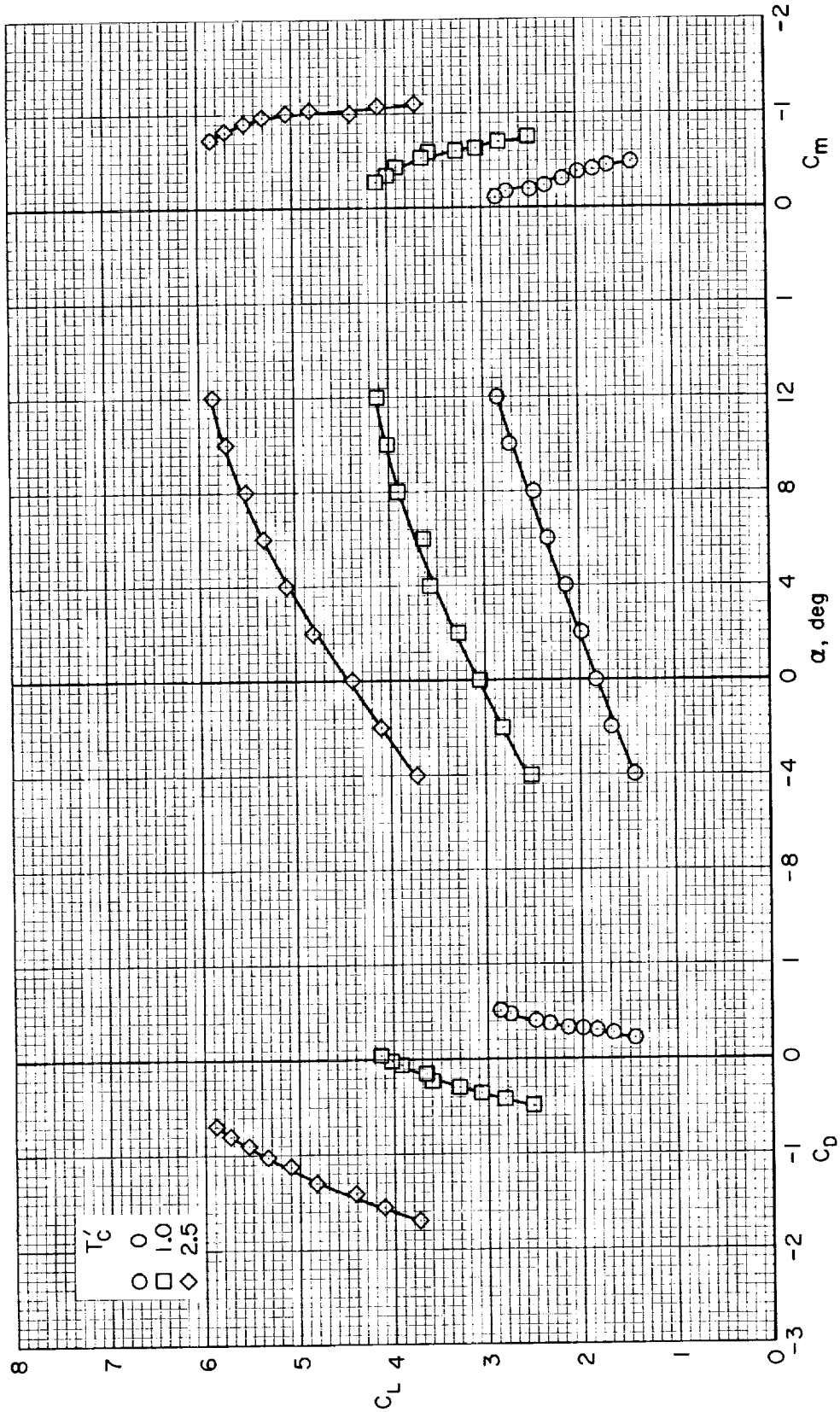

(c) $\delta_f = 100/60°$

Figure 8.- Concluded.

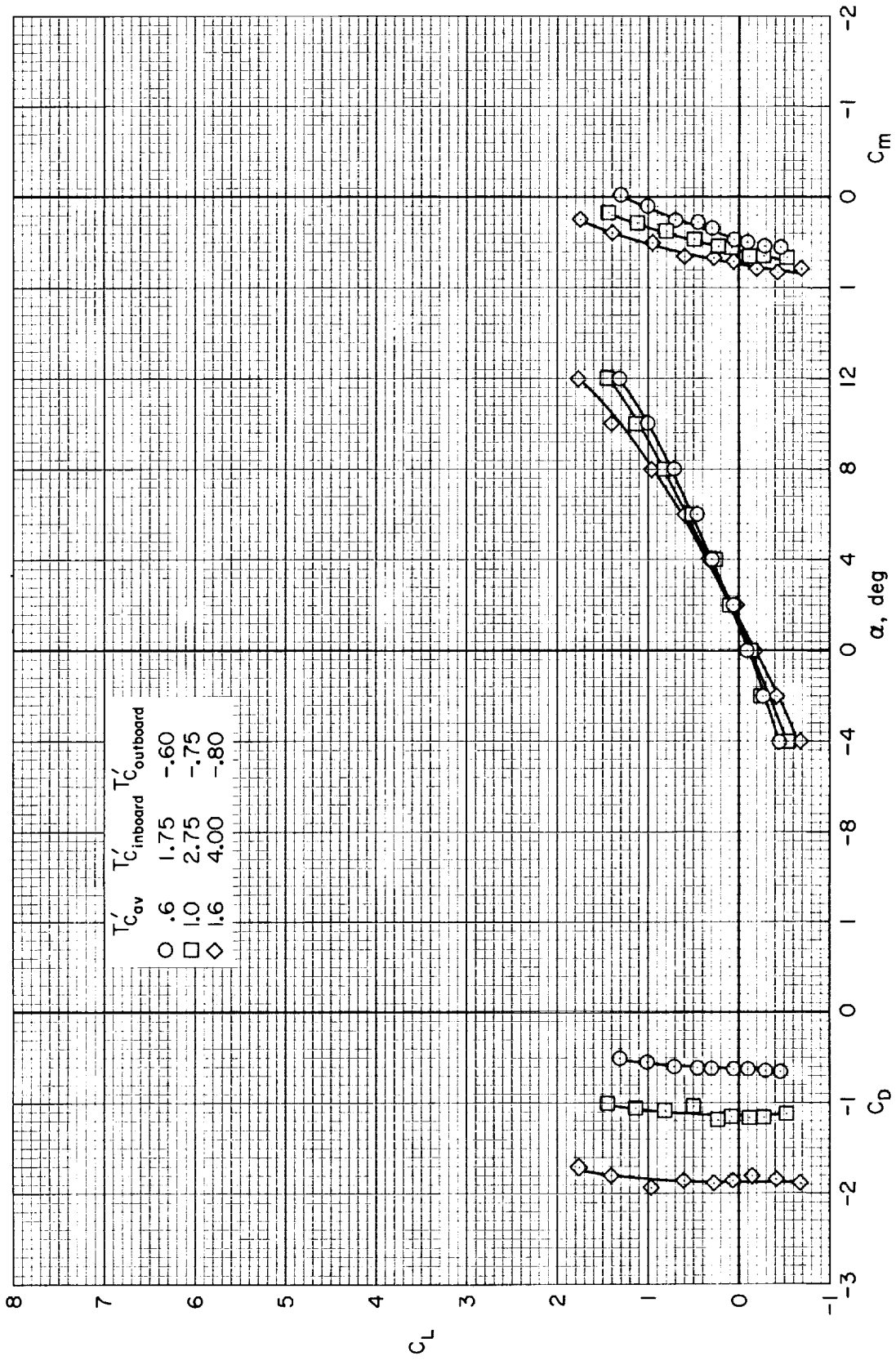

(a) $\delta_f = 0°$

Figure 9.- Effect of differential spanwise propeller thrust on the longitudinal characteristics of the model with medium-span wing, slats off; $\beta = 16/0°$, low horizontal tail.

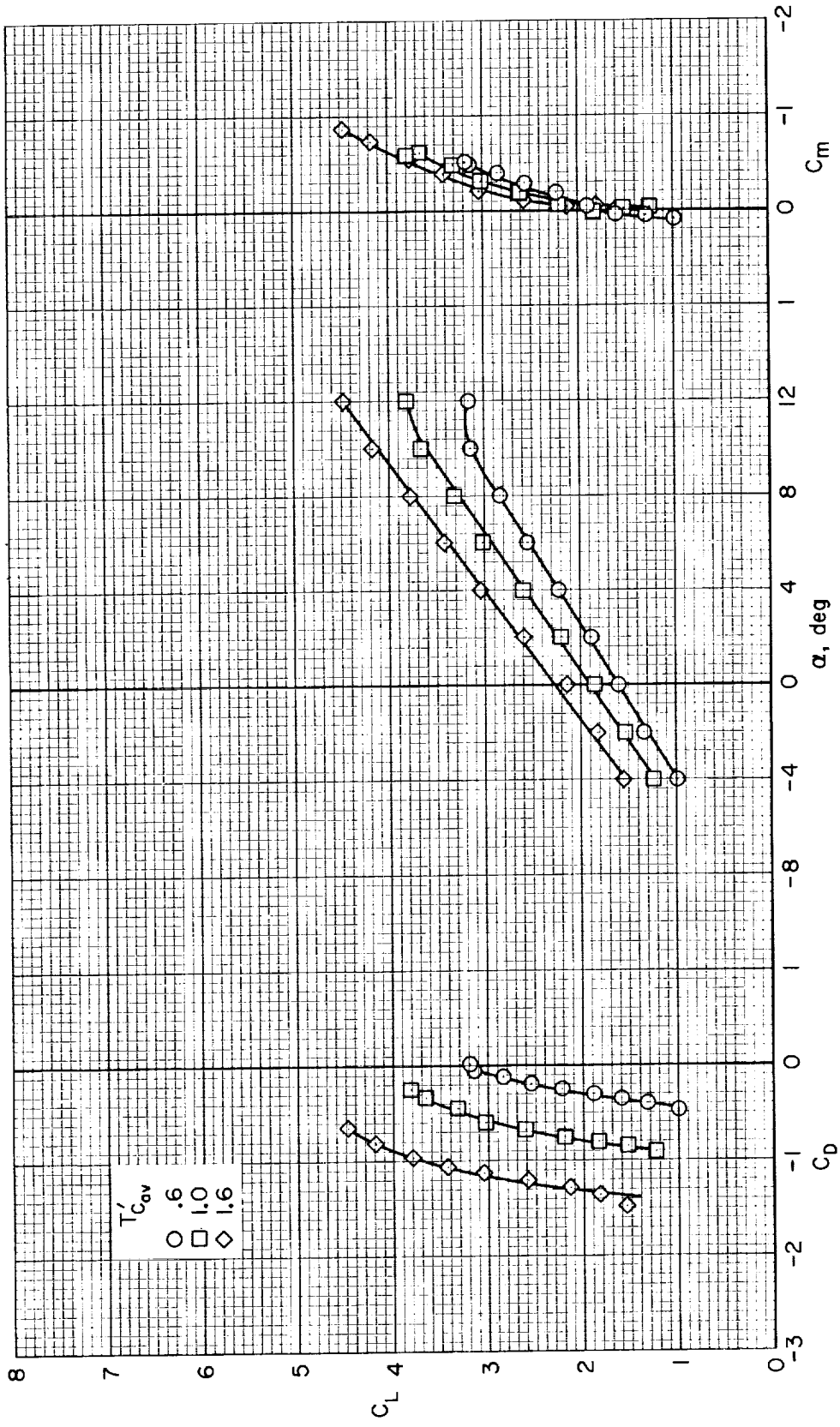

(b) $\delta_f = 40°$

Figure 9.- Continued.

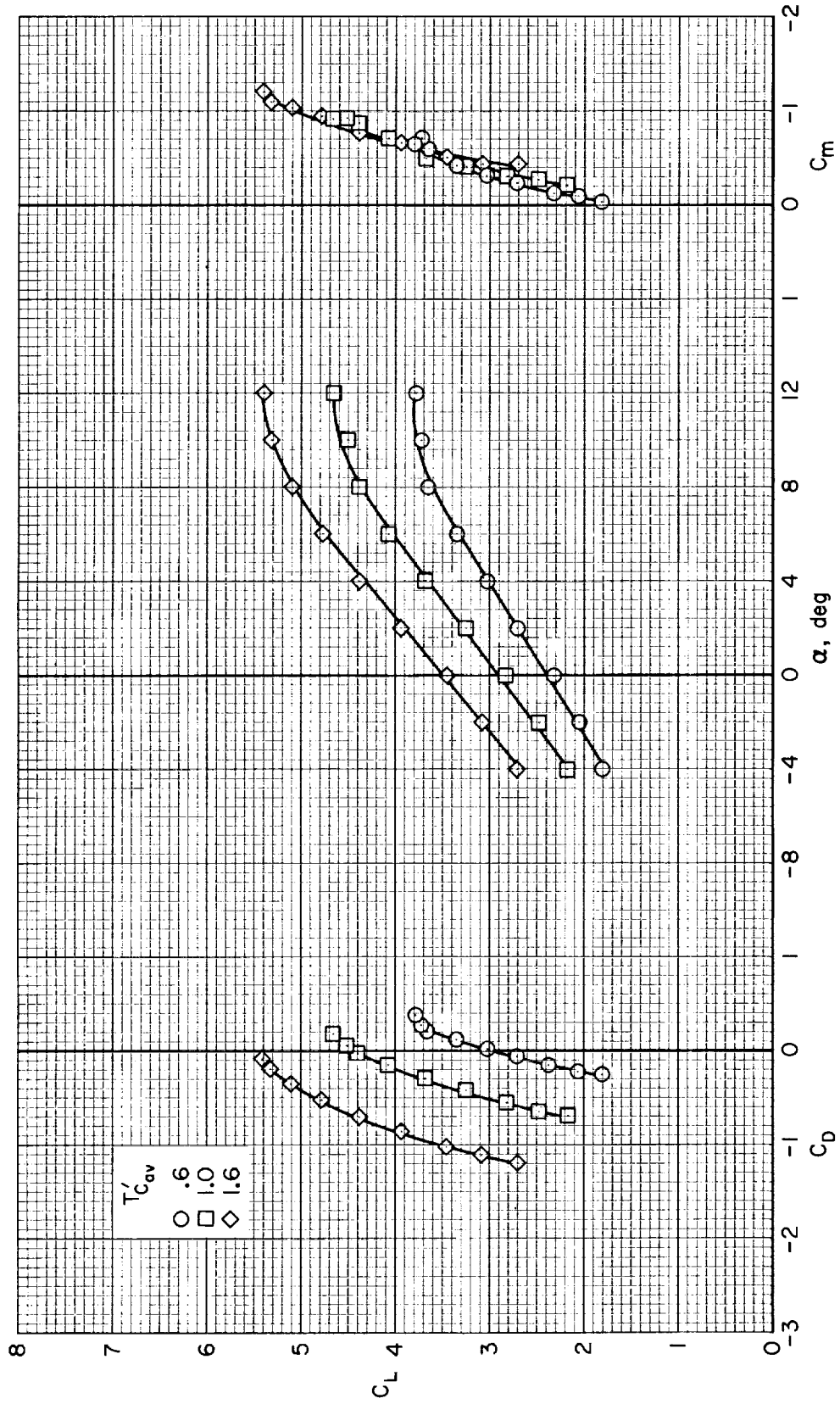

(c) $\delta_f = 60/40°$

Figure 9.- Continued.

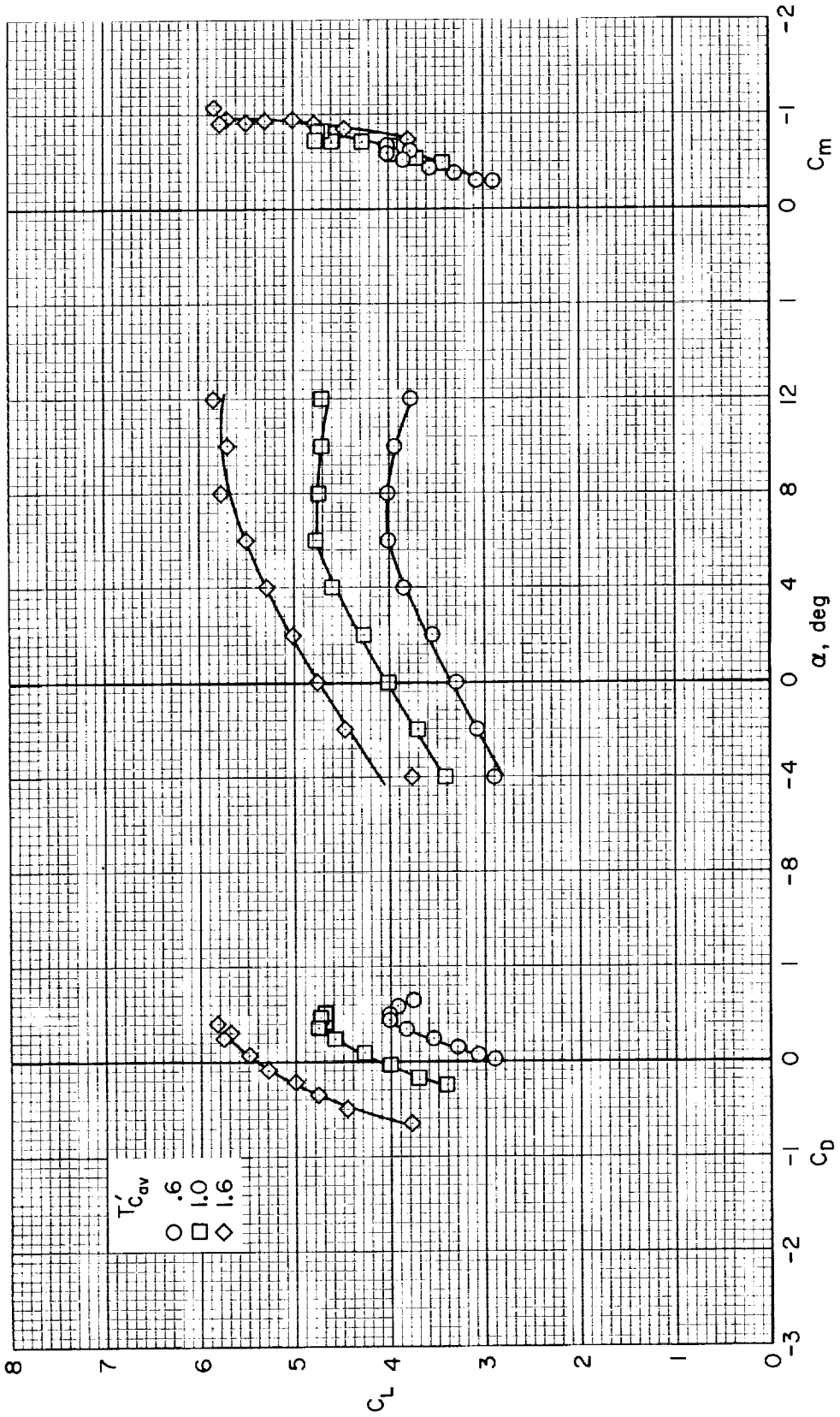

(d) $\delta_f = 80°$

Figure 9.- Continued.

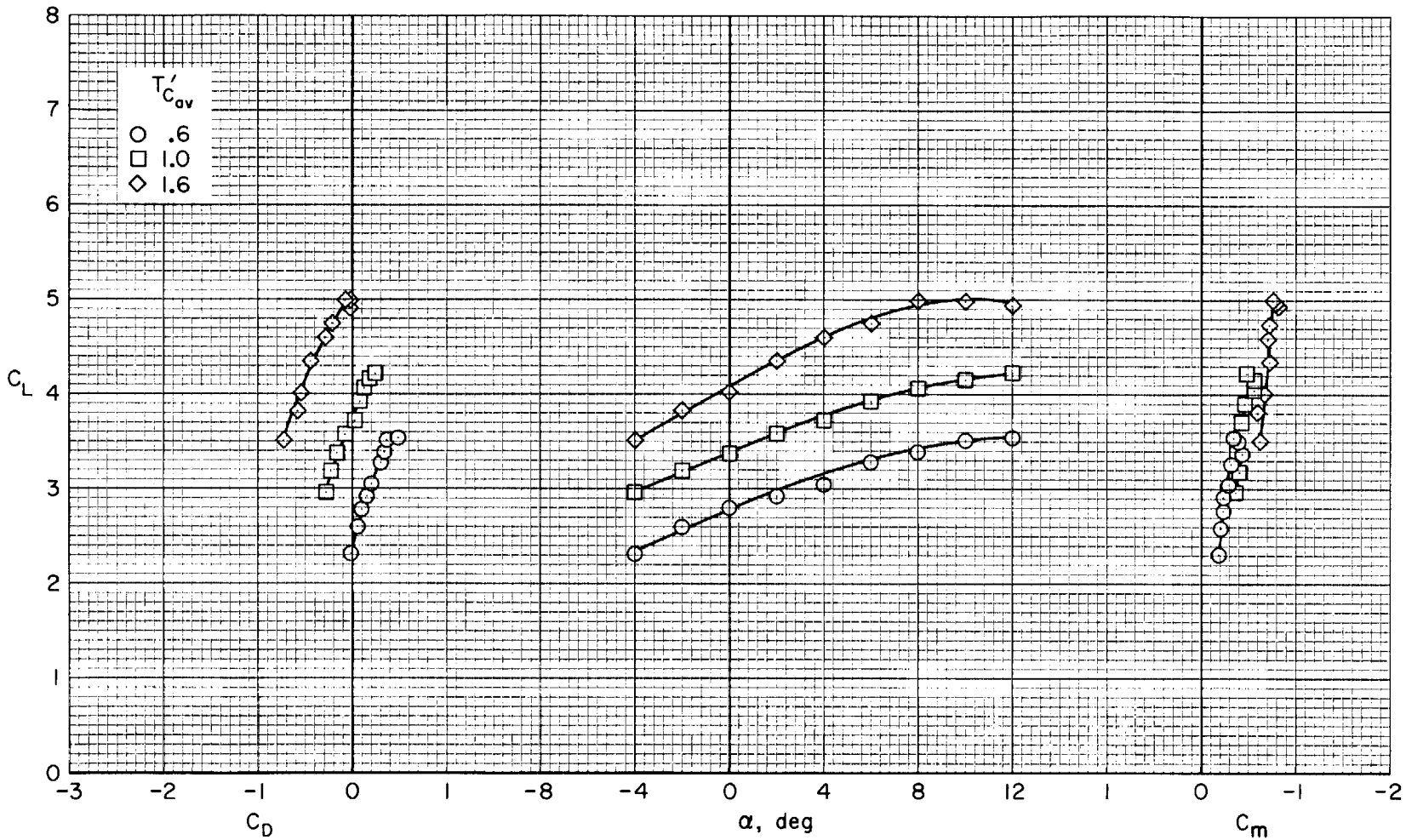

(e) $\delta_f = 100/60°$

Figure 9.- Concluded.

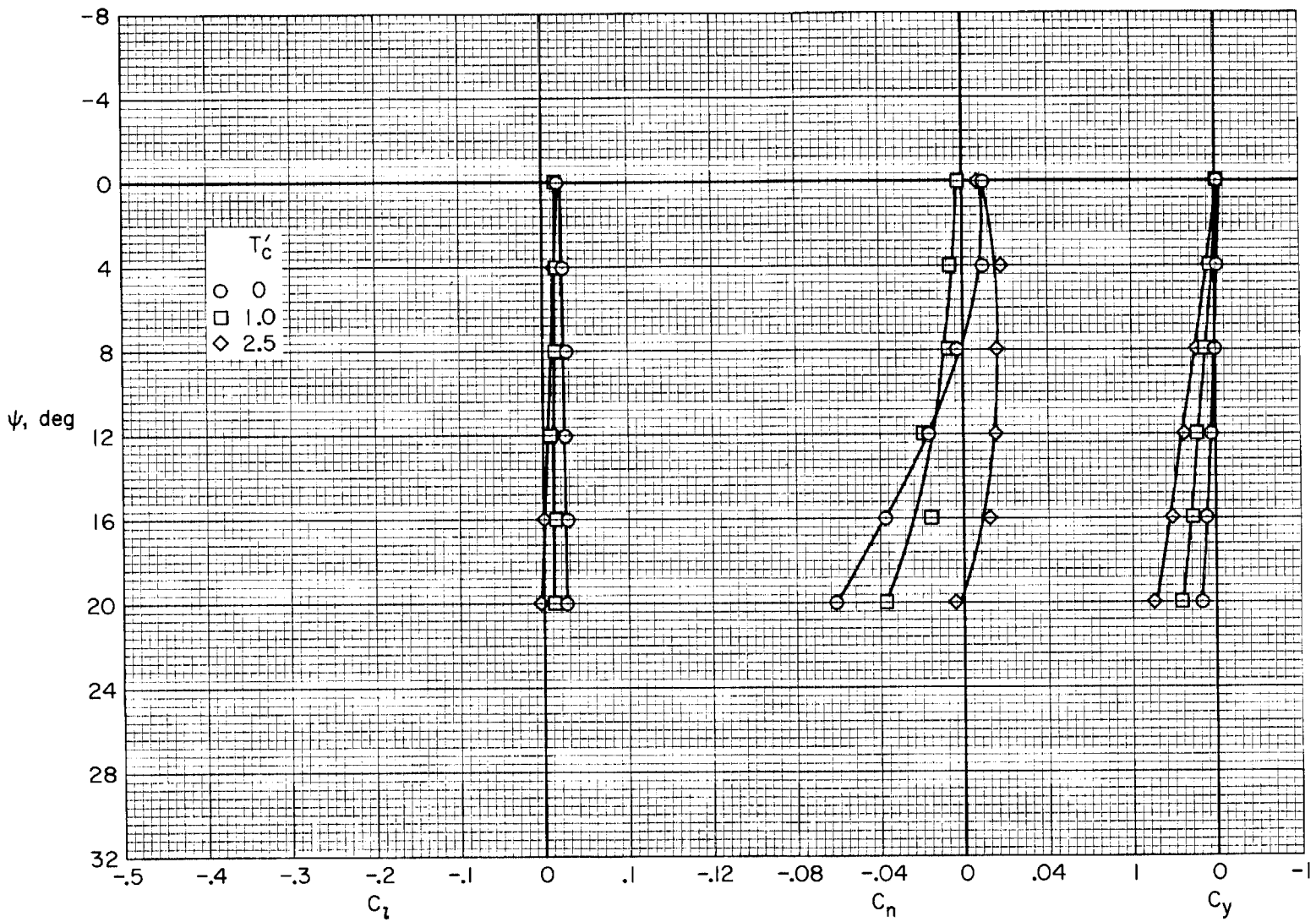

(a) Slats off.

Figure 10.- Effect of leading-edge slats on the lateral-directional characteristics of the model with short-span wing, tail off; $\delta_f = 100/60°$, $\beta = 16°$.

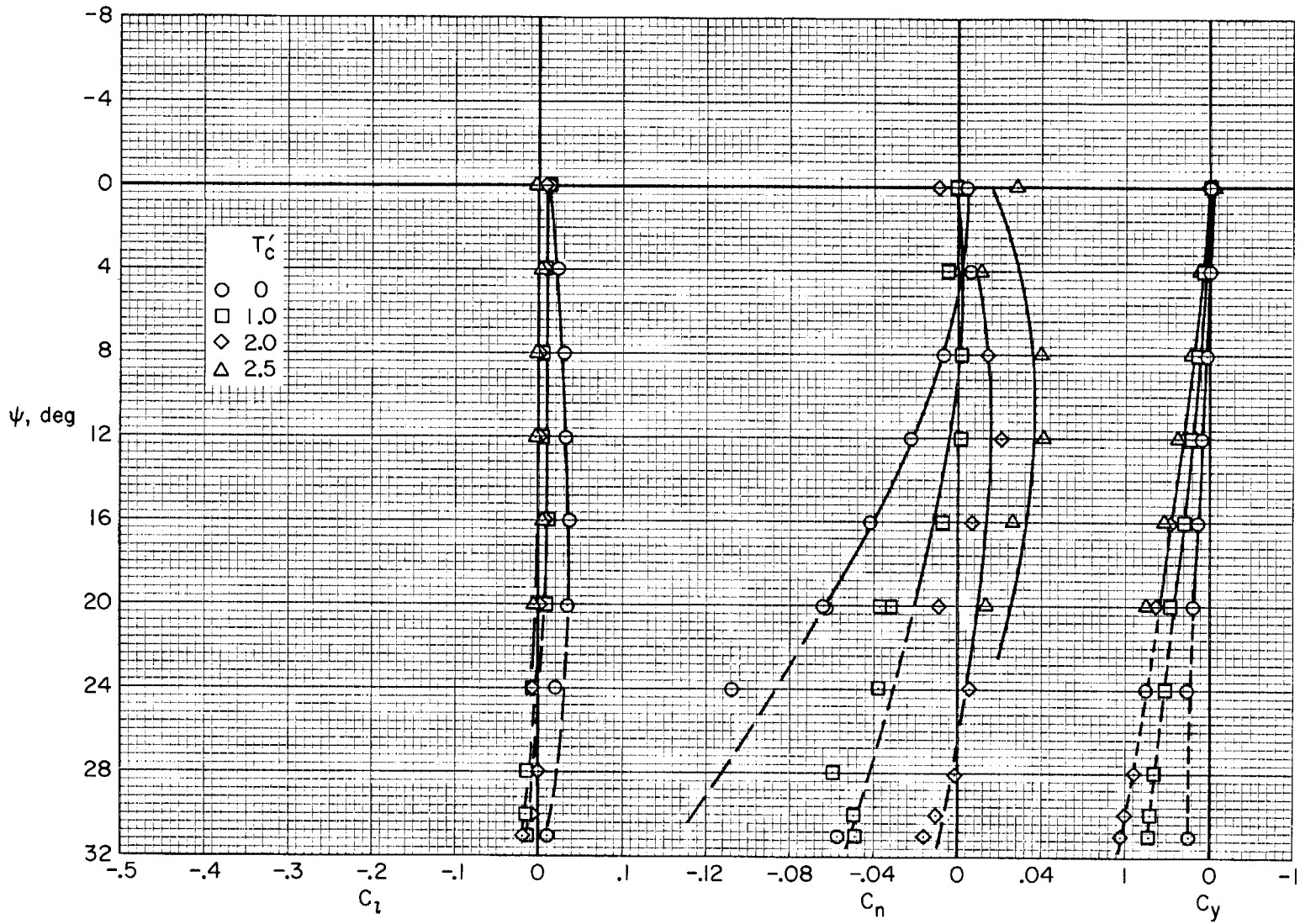

(b) Slats on.

Figure 10.- Concluded.

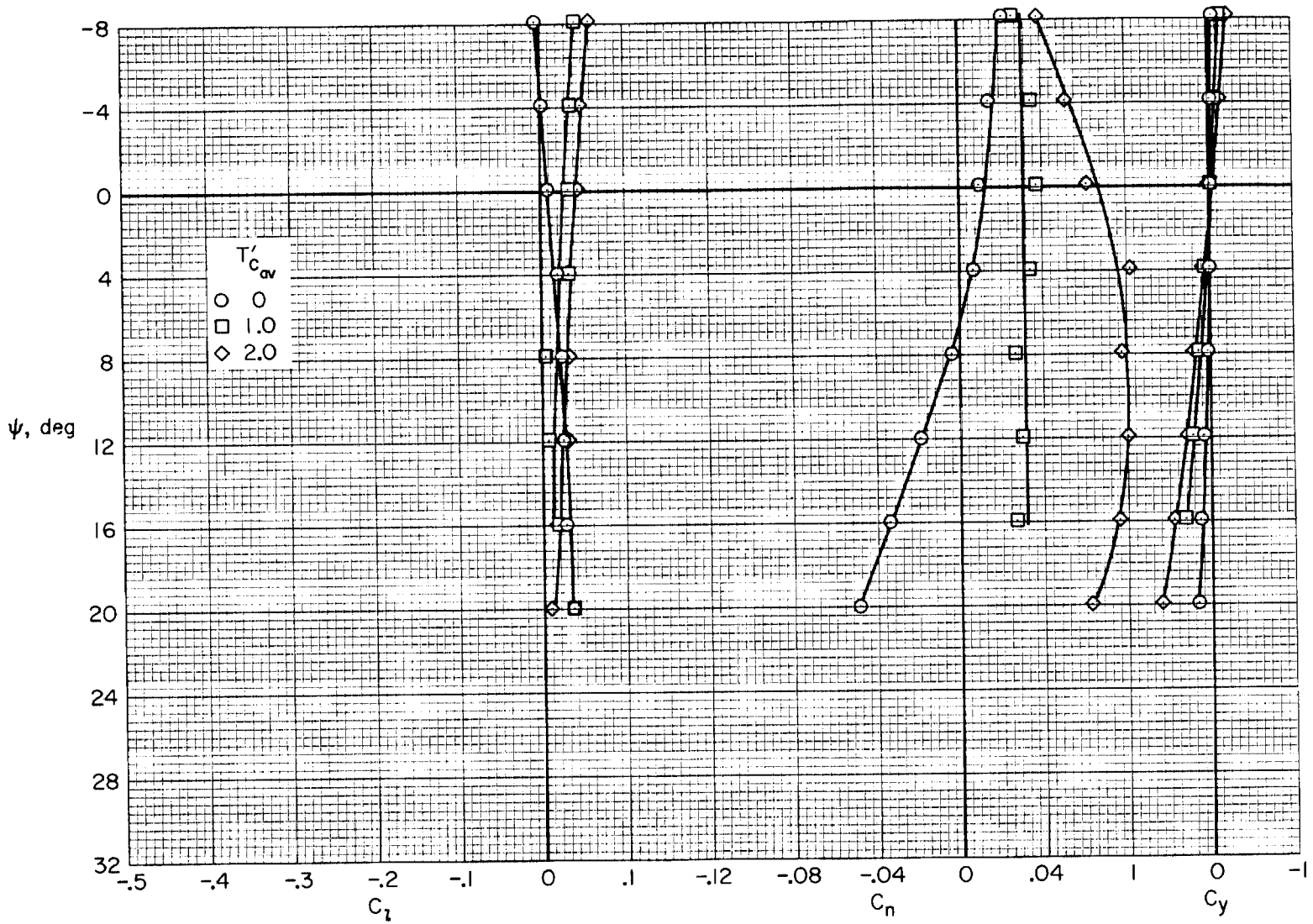

(a) $+\Delta\beta = 4°$ ($\beta = 18°/16°/16°/14°$)

Figure 11.- Effect of differential propeller pitch on the lateral-directional characteristics of the model with the short-span wing, tail off; $\delta_f = 100/60°$, slats on.

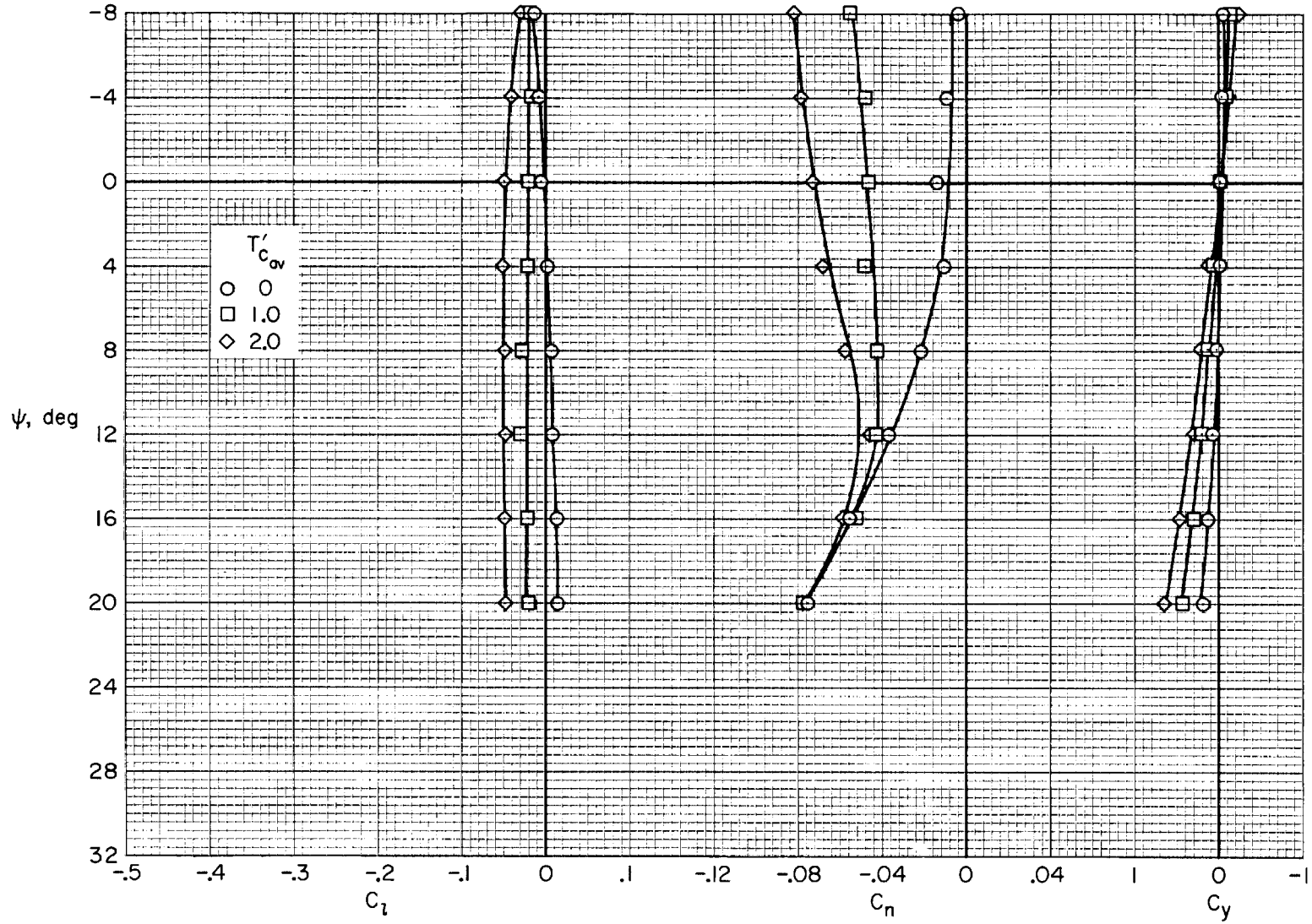

(b) $-\Delta\beta = 4°$ ($\beta = 14°$/ 18°)

Figure 11.- Concluded.

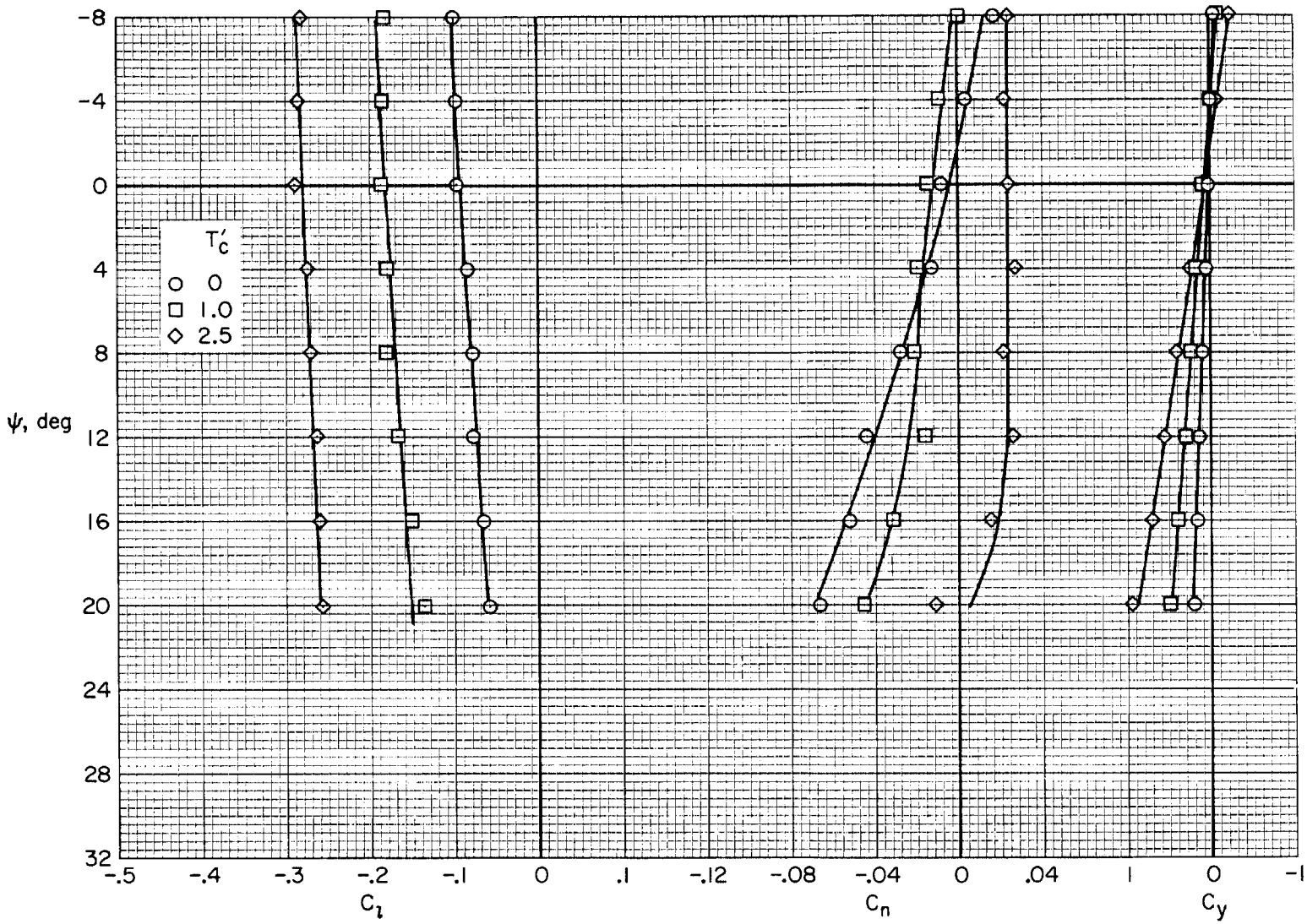

(a) $\delta_{sla} = 20°$

Figure 12.- Effect of 0.1c slot-lip aileron on lateral-directional characteristics of the model with short-span wing, tail off, slats on; $\delta_f = 100/60°$.

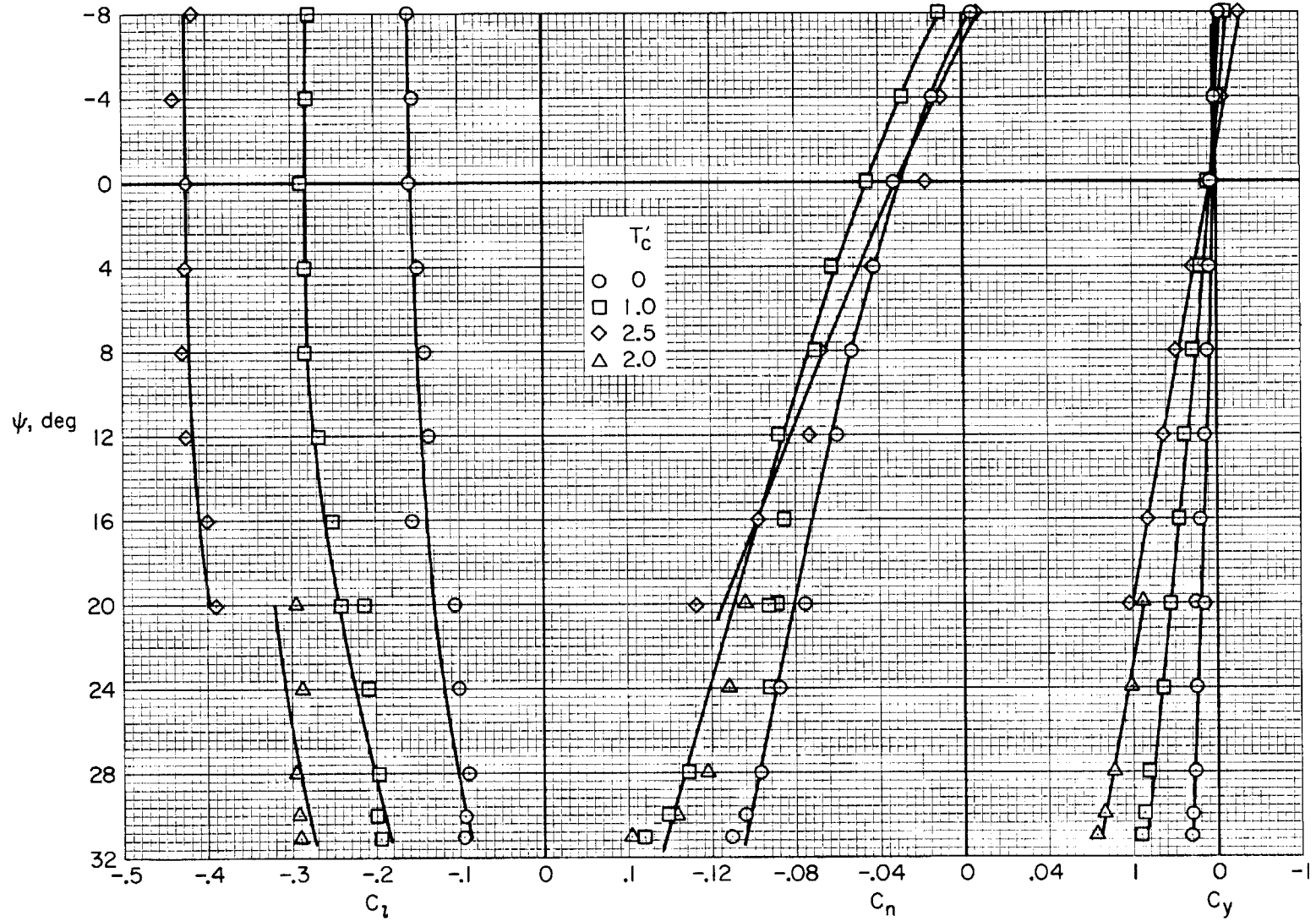

(b) $\delta_{sla} = 60°$

Figure 12.- Concluded.

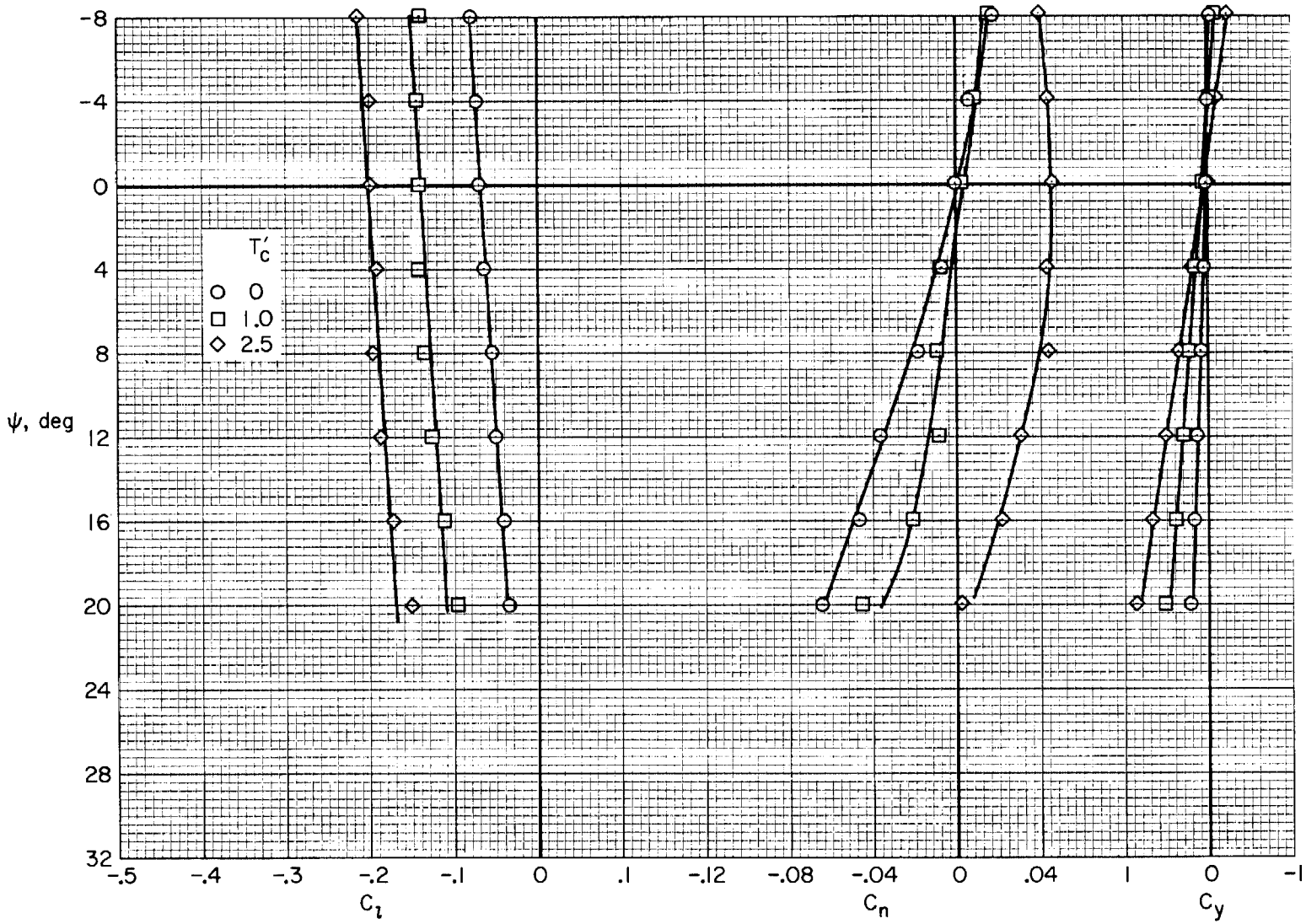

(a) $\delta_s = 20°$

Figure 13.- Effect of spoiler on lateral-directional characteristics of the model with short-span wing, tail off, slats on; $\delta_f = 100/60°$; 0.1c spoiler.

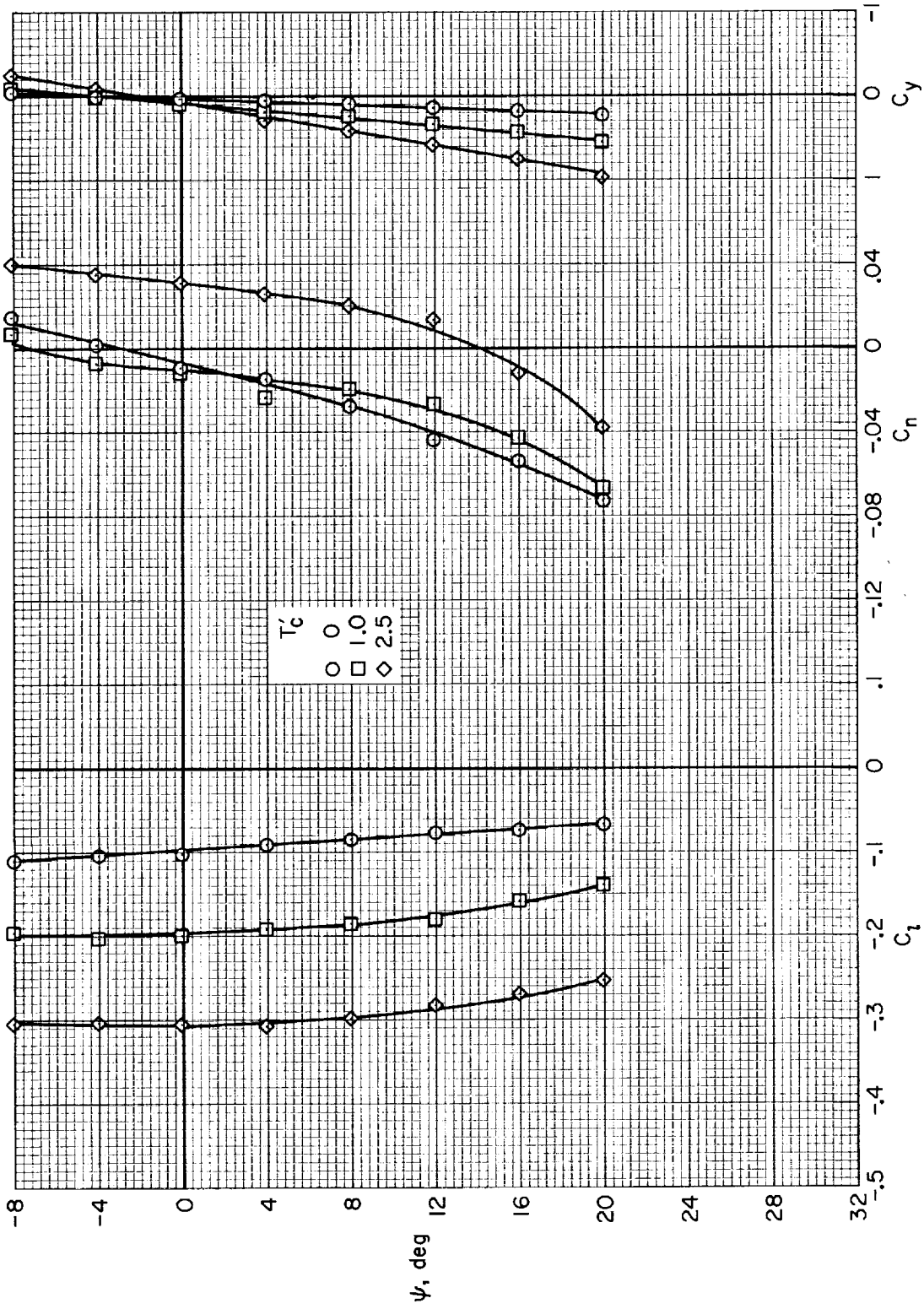

(b) $\delta_s = 40°$

Figure 13. - Concluded.